ANNALES MATHÉMATIQUES

BLAISE PASCAL

Mohamed Aït-Nouh,
Daniel Matignon and Kimihiko Motegi

Geometric types of twisted knots

Volume 13, n° 1 (2006), p. 31-85.

<http://ambp.cedram.org/item?id=AMBP_2006__13_1_31_0>

Publication éditée par les laboratoires de mathématiques
de l'université Blaise-Pascal, UMR 6620 du CNRS
Clermont-Ferrand — France

cedram

Article mis en ligne dans le cadre du
Centre de diffusion des revues académiques de mathématiques
http://www.cedram.org/

Annales mathématiques Blaise Pascal **13**, 31-85 (2006)

Geometric types of twisted knots

Mohamed Aït-Nouh
Daniel Matignon
Kimihiko Motegi

Abstract

Let K be a knot in the 3-sphere S^3, and Δ a disk in S^3 meeting K transversely in the interior. For non-triviality we assume that $|\Delta \cap K| \geq 2$ over all isotopies of K in $S^3 - \partial\Delta$. Let $K_{\Delta,n}(\subset S^3)$ be a knot obtained from K by n twistings along the disk Δ. If the original knot is unknotted in S^3, we call $K_{\Delta,n}$ a *twisted knot*. We describe for which pair (K, Δ) and an integer n, the twisted knot $K_{\Delta,n}$ is a torus knot, a satellite knot or a hyperbolic knot.

1. Introduction

Let K be a knot in the 3-sphere S^3 and Δ a disk in S^3 meeting K transversely in the interior. We assume that $|\Delta \cap K|$, the number of $\Delta \cap K$, is minimal and greater than one over all isotopies of K in $S^3 - \partial\Delta$. We call such a disk Δ a *twisting disk* for K. Let $K_{\Delta,n}(\subset S^3)$ be a knot obtained from K by n twistings along the disk Δ, in other words, an image of K after a $-\frac{1}{n}$-Dehn surgery on the trivial knot $\partial\Delta$. In particular, if K is a trivial knot in S^3, then we call (K, Δ) a *twisting pair* and call $K_{\Delta,n}$ a *twisted knot*, see Figure 1.

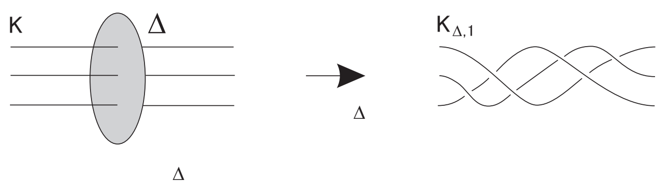

Figure 1

Let $\mathcal{K}$ be the set of all knots in S^3 and $\mathcal{K}_1$ the set of all twisted knots. In [23, Theorem 4.1] Ohyama demonstrated that each knot in $\mathcal{K}_2 = \mathcal{K} - \mathcal{K}_1$ can be obtained from a trivial knot by twisting along exactly two properly chosen disks.

On the other hand, following Thurston's uniformization theorem ([20, 28]) and the torus theorem ([14, 15]), every knot in S^3 has exactly one of the following *geometric types*:
a torus knot, a satellite knot (i.e., a knot having a non-boundary-parallel, incompressible torus in its exterior), or a hyperbolic knot (i.e., a knot admitting a complete hyperbolic structure of finite volume on its complement).

Let k be a knot in $\mathcal{K}_1$, then $k = K_{\Delta,n}$, for some twisting pair (K, Δ) and an integer n. Let c be the boundary of the twisting disk, $c = \partial\Delta$ and $E(K, c) = S^3 - \mathrm{int}N(K \cup c)$. Since $E(K, c)$ is irreducible and ∂-irreducible, $E(K, c)$ is Seifert fibered, toroidal or hyperbolic ([14, 15, 20, 28]). Thus each twisting pair (K, Δ) has also exactly one of the following *geometric types*: is *Seifert fibered* type, *toroidal* type or *hyperbolic* type according to whether $E(K, c)$ is Seifert fibered, toroidal or hyperbolic, respectively.

In the present paper, we address:

Problem 1.1. *Describe geometric types of twisted knots with respect to geometric types of the twisting pairs and the twisting numbers.*

Actually, we shall prove:

Theorem 1.2. *Let (K, Δ) be a twisting pair and n an integer. If $\mid n \mid> 1$ then $K_{\Delta,n}$ has the geometric type of (K, Δ).*

For hyperbolic twisting pairs, the result is a consequence of Proposition 1.3 below, [19] and [2, Theorem 1.1]. It should be mentioned that Proposition 1.3 can be deduced from a more general result [12, Appendix A.2] established by Gordon and Luecke; notice that their proof is based on *good and binary faces*, whereas our proof is based on *primitive or binary faces*; see the end of Section 3 for more details.

Proposition 1.3. *Let (K, Δ) be a hyperbolic, twisting pair. If $K_{\Delta,n}$ is a satellite knot for some integer n with $|n| \geq 2$, then $K_{\Delta,n}$ is a cable of a torus knot and $|n| = 2$.*

Proof of Theorem 1.2 for hyperbolic twisting pairs. Let (K, Δ) be a hyperbolic twisting pair. Assume that $|n| > 1$. By [19], $K_{\Delta,n}$ is not a torus knot. If $K_{\Delta,n}$ is a satellite knot, then by Proposition 1.3, it would be a cable of a torus knot. This contradicts [2, Theorem 1.1] which asserts that $K_{\Delta,n}$ ($|n| > 1$) cannot be a graph knot. Thus $K_{\Delta,n}$ is a hyperbolic knot. $\square$

If (K, Δ) is a Seifert fibered pair, then $S^3 - \mathrm{int}N(\partial\Delta)$ is a $(1, p)$-fibered solid torus in which K is a regular fiber. Hence $K_{\Delta,n}$ is a $(1+np, p)$-torus knot in S^3. Thus we have:

Proposition 1.4. *Let (K, Δ) be a Seifert fibered twisting pair. Then $K_{\Delta,n}$ is a torus knot for any integer n.*

For toroidal twisting pairs, we have the following precise description.

Theorem 1.5. *Let (K, Δ) be a toroidal twisting pair.*

(1) (i) *If (K, Δ) has a form described in Figure 2* (i) *in which $V - \mathrm{int}N(K)$ is Seifert fibered or hyperbolic, then $K_{\Delta,n}$ is a satellite knot for any integer $n \neq 0, -1$; $K_{\Delta,-1}$ is a torus knot or a hyperbolic knot, respectively.*
(ii) *If (K, Δ) has a form described in Figure 2* (ii) *in which $V - \mathrm{int}N(K)$ is Seifert fibered or hyperbolic, then $K_{\Delta,n}$ is a satellite knot for any integer $n \neq 0, 1$; $K_{\Delta,1}$ is a torus knot or a hyperbolic knot, respectively.*

(2) *If (K, Δ) has a form other than those in* (1)*, then $K_{\Delta,n}$ is a satellite knot for any non-zero integer n.*

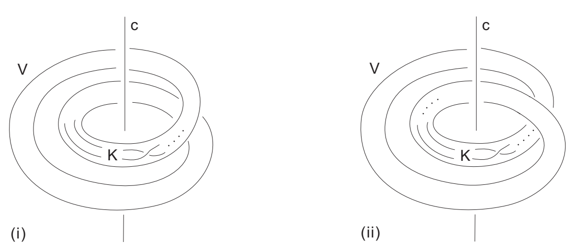

FIGURE 2

Let us now give some examples of hyperbolic twisting pairs (K, Δ) such that $K_{\Delta,1}$ is not a hyperbolic knot. By taking the mirror image of the pair, we can obtain a hyperbolic twisting pair $(\bar{K}, \bar{\Delta})$ such that $\bar{K}_{\bar{\Delta},-1}$ is not a hyperbolic knot.

Example 1 (Producing torus knots from hyperbolic pairs).

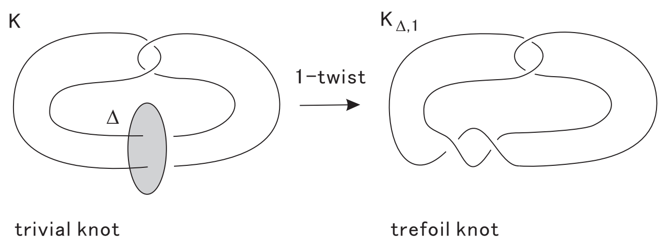

Figure 3

In Figure 1, (K, Δ) is a hyperbolic pair, but $K_{\Delta,1}$ is a trefoil knot. In [5, Theorem 1.3], [29, p.2293], we find other examples of hyperbolic pairs (K, Δ) such that $K_{\Delta,1}$ is a torus knot.

Example 2 (Producing satellite knots from hyperbolic pairs).

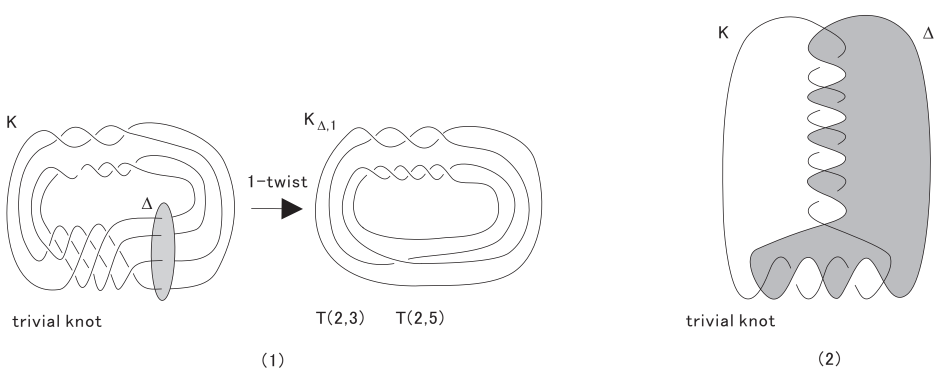

Figure 4

In Figure 4 (1) $K_{D,1}$ is a connected sum of two torus knots [22]; we found examples of composite twisted knots in [6, 27].

In Figure 4 (2), (K, Δ) is a hyperbolic pair ([18]), but $K_{\Delta,1}$ is a $(23, 2)$-cable of a $(4, 3)$-torus knot [5, Theorem 1.4], [29].

Every known satellite twisted knot has a special type: a connected sum of a torus knot and some prime knot, or a cable of a torus knot. So we would like to ask:

Question. Let (K, Δ) be a hyperbolic, twisting pair. If the resulting twisted knot is satellite, then is it a connected sum of a torus knot and some prime knot, or a cable of a torus knot?

In the proof of Proposition 1.3, we will use the *intersection graphs*, which come from a meridian disk of the solid torus $S^3 - \mathrm{int}N(K)$ and an essential 2-torus in $S^3 - \mathrm{int}N(K_{D,n})$. In Section 3 we will define the pair of graphs and prepare some terminologies. The sketch of the proof of Proposition 1.3 will be given there. The results of this paper has been announced in [1].

2. Twistings on non-hyperbolic twisting pairs

In this section we prove Theorem 1.5.

Proof. Let T be an essential torus in $S^3 - \mathrm{int}N(K \cup c)$, where $c = \partial\Delta$. Then there are two possibilities:

- T does not separate $\partial N(K)$ and $\partial N(c)$,
- T separates $\partial N(K)$ and $\partial N(c)$.

Case 1 – T does not separate $\partial N(K)$ and $\partial N(c)$.
Let V be a solid torus bounded by T ([24, p.107]). Since T is essential in $S^3 - \mathrm{int}N(K \cup c)$, K and c are contained in V and V is knotted in S^3. Furthermore, since K (resp. c) is unknotted in S^3, there is a 3-ball B_K (resp. B_c) in V which contains K (resp. c) in its interior; but there is no 3-ball in V which contains $K \cup c$.

Since $c \subset B_c \subset V$, we have a meridian disk D_V of V such that $c \cap D_V = \emptyset$. Then the algebraic intersection number of $K_{\Delta,n}$ and a meridian disk D_V of V coincides with that of K and D_V, which is zero, because that $K \subset B_K$. Therefore, $K_{\Delta,n}$ is not a core of V.

Since V is knotted in S^3, the claim below shows that $K_{\Delta,n}$ is a satellite knot with a companion knot ℓ (the core of V) for any non-zero integer n.

Lemma 2.1. *$K_{\Delta,n}$ is not contained in a 3-ball in V for any non-zero integer n.*

Proof. Let M be a 3-manifold $V - \mathrm{int}N(K)$. Then $M - \mathrm{int}N(c) = V - \mathrm{int}N(K \cup c)$ is irreducible and boundary-irreducible. Assume for a contradiction that $K_{\Delta,n}$ is contained in a 3-ball in V for some non-zero integer n. Then $M(c; -\frac{1}{n}) \cong V - \mathrm{K_{\Delta,n}}$ is reducible. Then from [26, Theorem 6.1], we see that c is cabled and the surgery slope $-\frac{1}{n}$ is the slope of the cabling annulus, which is an integer p such that $\mid p \mid \geq 2$, a contradiction. Thus $K_{\Delta,n}$ is not contained in a 3-ball in V for any non-zero integer n. $\square$

Case 2 – T separates $\partial N(K)$ and $\partial N(c)$.
The torus T cuts S^3 into two 3-manifolds V and W. Without loss of generality, we may assume that $K \subset V$, $c \subset W$. Now we show that V is an unknotted solid torus in S^3. The solid torus theorem [24, p.107] shows that V or W is a solid torus. Suppose first that V is a solid torus. Since T is essential in $S^3 - \mathrm{int}N(K \cup c)$, K is not contained in a 3-ball in V and not a core of V. Furthermore, since K is unknotted in S^3, V is unknotted in S^3. If W is a solid torus, then since c is also unknotted in S^3, the above argument shows that W is unknotted in S^3, and hence V is also an unknotted solid torus. Let ℓ be a core of V. Since T is essential in $S^3 - \mathrm{int}N(K \cup c)$ (because T is not parallel to $\partial N(c)$), ℓ intersects the twisting disk Δ more than once: (ℓ, Δ) is also a twisting pair.

If $\ell_{\Delta,n}$ is knotted in S^3, then $K_{\Delta,n}$ is a satellite knot with a companion knot $\ell_{\Delta,n}$. Assume that $\ell_{\Delta,n}$ is unknotted in S^3 for some non-zero integer n. Then from [17, Corollary 3.1], [16, Theorem 4.2], we have the situation as in Figure 2 (i) and $n = -1$, or Figure 2 (ii) and $n = 1$.

In either case, we have:

Lemma 2.2. *For any toroidal pair (K, Δ), $K_{\Delta,n}$ is a satellite knot if $|n| > 1$.*

Suppose that (K, Δ) is a pair shown in Figure 2 (i) (resp.(ii)). Since $\ell_{\Delta,-1}$ (resp. $\ell_{\Delta,1}$) is also unknotted in S^3 and the linking number of ℓ and $\partial\Delta$ is two, we see that $K_{\Delta,-1}$ (resp. $K_{\Delta,1}$) can be regarded as the result of -4-twist (resp. 4-twist) along the meridian disk D_V of V:

$$K_{\Delta,-1} = K_{D_V,-4} \quad (\text{resp. } K_{\Delta,1} = K_{D_V,4}).$$

If $V - \mathrm{int}N(K)$ is neither Seifert fibered nor hyperbolic, i.e., $V - \mathrm{int}N(K)$ is toroidal, then by Lemma 2.2, $K_{\Delta,-1} = K_{D_V,-4}$ (resp. $K_{\Delta,1} = K_{D_V,4}$) is a satellite knot. This completes the proof of Theorem 1.5 (2).

Suppose that (K, Δ) is a pair shown in Figure 2 (i) (resp. (ii)) in which $V - \mathrm{int}N(K)$ is Seifert fibered or hyperbolic. As we mentioned above, except for $n = -1$ (resp. $n = 1$) $\ell_{\Delta,n}$ is knotted and $K_{\Delta,n}$ is a satellite knot. To finish the proof we consider the exceptional cases. If $V - \mathrm{int}N(K)$ is Seifert fibered, then $K_{\Delta,-1} = K_{D_V,-4}$ (resp. $K_{\Delta,1} = K_{D_V,4}$) is a torus knot by Proposition 1.4. If $V - \mathrm{int}N(K)$ is hyperbolic, then by Theorem 1.2 (for hyperbolic twisting pairs), $K_{\Delta,-1} = K_{D_V,-4}$ (resp. $K_{\Delta,1} = K_{D_V,4}$) is a hyperbolic knot. $\square$

3. Twistings on hyperbolic twisting pairs

Assume that (K, Δ) is a hyperbolic twisting pair and $K_{\Delta,n}$ is non-hyperbolic. Then $K_{\Delta,n}$ is a torus knot or a satellite knot. If $K_{\Delta,n}$ is a torus knot, then [21, Theorem 3.8] (which was essentially shown in [19]) shows that $|n| \leq 1$.

So in the following, we assume that $K_{\Delta,n}$ is a satellite knot.

For notational convenience, we set $c = \partial\Delta$ and $K_n = K_{\Delta,n}$. Let M be the exterior $S^3 - \mathrm{int}N(K \cup c)$, and $M(r)$ the manifold obtained by r-Dehn filling along $\partial N(c)$. Then we have $M(1/0) \cong S^3 - \mathrm{int}N(K) \cong S^1 \times D^2$ and $M(-1/n) \cong S^3 - \mathrm{int}N(K_n)$. We denote the image of c in $M(-1/n)$ by c_n, so that $c_0 = c \subset M(1/0)$ and $c_n \subset M(-1/n)$.

Let $\hat{D}$ be a meridian disk of $M(1/0)$. Isotope $\hat{D}$ so that the number of components $|\hat{D} \cap N(c)| = q$ is minimal among meridian disks of $M(1/0)$. If $q = 0$, then $K \cup c$ would be a split link contradicting the hyperbolicity of $K \cup c$. If $q = 1$, then $K \cup c$ is a Hopf link contradicting again the hyperbolicity of $K \cup c$. Henceforth we assume that $q \geq 2$.

Put $D = \hat{D} \cap M$, which is a punctured disk, with q *inner boundary components* each of which has slope $1/0$ on $\partial N(c)$, and a single *outer boundary component* $\partial\hat{D}$.

Since K_n is a satellite knot, the exterior $S^3 - \mathrm{int}N(K_n) = M(-1/n)$ contains an essential torus $\hat{T}$. By the solid torus theorem [24, p.107] $\hat{T}$ bounds a solid torus V in S^3 containing K_n in its interior. The core of V

is denoted by ℓ, which is a non-trivial companion knot of K_n. Note that since $M = S^3 - \mathrm{int}N(K \cup c)$ is assumed to be hyperbolic, $\hat{T} \cap c_n \neq \emptyset$. We choose $\hat{T}$ so that $\hat{T} \cap N(c_n)$ is a union of meridian disks and $|\hat{T} \cap N(c_n)| = t$ is minimal. Since $\hat{T}$ is separating, $t (\neq 0)$ is an even integer.

Let $T = \hat{T} \cap M$ be a punctured torus, with t boundary components each of which has slope $-1/n$ on $\partial N(c)$.

We assume further that D and T intersect transversely and ∂D and ∂T intersect in the minimal number of points so that each inner boundary component of D intersects each boundary component of T in exactly $|n|$ points on $\partial N(c)$.

Lemma 3.1. *The surfaces D and T are essential in M.*

Proof. The minimality of q implies that D is essential in M. Since $\hat{T}$ is essential in $M(-1/n)$ and t is minimal, T is also essential in M. □

Let us define two associated graphs G_D and G_T on $\hat{D}$ and $\hat{T}$ respectively, in the usual way (see [7] for more details). We recall some definitions. The (fat) *vertices* of G_T (resp. G_D) are the disks $\hat{T} - \mathrm{int}T$ (resp. $\hat{D} - \mathrm{int}D$). The *edges* of G_T (resp. G_D) are the arc components of $D \cap T$ in $\hat{T}$ (resp. in $\hat{D}$). We number the components of ∂T by $1, 2, \ldots, t$ in the order in which they appear on $\partial N(c)$. Similarly, we number $1, 2, \ldots, q$ the inner boundary components of D. This gives a numbering of the vertices of G_D and G_T. Furthermore, it induces a labelling of the endpoints of the edges: the label at one endpoint of an edge in one graph corresponds to the number of the boundary component of the other surface (the vertex of the other graph) that contains this endpoint. We next give a *sign*, $+$ or $-$, to each vertex of G_D (resp. G_T), according to the direction on $\partial N(c) \subset M$ of the orientation of the corresponding boundary component of D (resp. T), induced by some chosen orientation of D (resp. T). Two vertices on G_D (resp. G_T) are said to be *parallel* if they have the same sign, in other words, the corresponding boundaries of D (resp. T) are homologous on $\partial N(c)$; otherwise the vertices are said to be *antiparallel*.

To prove Proposition 1.3, in what follows, we assume that the twisted knot K_n is a satellite knot for some n with $|n| \geq 2$. Since $M(1/0)$ is a solid torus and $M(-1/n) = E(K_n)$ is a toroidal manifold, from Theorems 1.1 and 6.1 in [11] we may assume that $|n| = \Delta(\frac{-1}{n}, \frac{1}{0}) = 2$, and that $t = 2$.

Let V_1 and V_2 be the two vertices of G_T; they have opposite signs, because T is separating. Since T is incompressible, by cut and paste arguments, we may assume that there is no circle component of $T \cap D$, which bounds a disk in D. Therefore we can divide the faces of G_D into the *black* faces and the *white* faces, according to the face is in V or $S^3 - V$, respectively.

Definition (great web) A connected subgraph Λ of G_D is a *web* if
(i) all the vertices of Λ have the same sign,
(ii) there are at most two edge-endpoints where the fat vertices of Λ are incident to edges of G_D that are not edges of Λ. (We refer to such an edge as a *ghost edge* of Λ and the label of such an endpoint as a *ghost label.*)

Furthermore, if the web Λ satisfies the following condition, then we call Λ a *great web.*
(iii) Λ is contained in the interior of a disk $D_\Lambda \subset \hat{D}$ with the property that Λ contains all the edges of G_D that lie in D_Λ. See Figure 5.

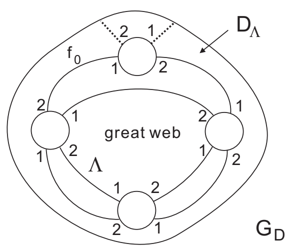

Figure 5

We recall the following fundamental result established by Gordon and Luecke.

Lemma 3.2 ([11])**.** *G_D contains a great web.*

Proof. Since $H_1(M(1/0)) \cong H_1(S^1 \times D^2)$ does not have a non-trivial torsion, G_T does not represent all types ([11, Theorem 2.2]) and therefore G_D contains a great web [11, Theorem 2.3]. $\square$

Let us take an innermost great web Λ in G_D and a disk D_Λ whose existence are assured by Lemma 3.2. Since Λ is connected, its faces are some disk faces and an annulus face f_0 ($f_0 \supset \partial\hat{D}$).

A vertex v is called a *boundary vertex* if $v \cap f_0 \neq \emptyset$; otherwise v is called an *interior vertex*. An edge e is called a *boundary edge* if $e \subset f_0$; otherwise e is called an *interior edge*. A disk face f of Λ is called an *interior face* if every vertex of f is an interior vertex.

A *Scharlemann cycle* is a cycle σ which bounds a disk face f (called a *Scharlemann disk*) whose vertices have the same sign and all the edges of σ have the same pair of consecutive labels $\{i, i+1\}$, so we refer to such a Scharlemann cycle as an $\{i, i+1\}$-Scharlemann cycle. Any Scharlemann cycle of G_D have the same labels $\{1, 2\}$. The number of the edges in σ is referred to as the *length* of the Scharlemann cycle σ or the *length* of the Scharlemann disk f. A *trivial loop* is an edge which bounds a disk face; i.e., a Scharlemann cycle of length one. By Lemma 3.1 G_D does not contain a trivial loop. In the following, a Scharlemann cycle is assumed to be of length at least two.

We recall the following from [10, Lemma 8.2]. Although the proof of [10, Lemma 8.2] works in our situation without changes, for convenience, we give a proof.

Lemma 3.3. *The graph G_D contains a black Scharlemann disk and a white Scharlemann disk; furthermore at least one of them has length* 2 *or* 3.

Proof. Since $t = 2$ and all the vertices of Λ have the same sign, the boundary of each disk face of Λ is a Scharlemann disk. Thus it is sufficient to show that there exist black and white disk faces in Λ. Let d be the number of vertices of Λ and E the number of edges of Λ. Since Λ has at most two ghost labels, $E \geq \frac{1}{2}(4d-2) = 2d-1$. Therefore an Euler-Poincaré characteristic calculus gives:

$$F = \sum_{f:\ face\ of\ \Lambda} \chi(f) = E - d + 1 \geq d$$

Note that since $\chi(f_0) = 0$, F coincides with number of disk faces of Λ. Since G_D contains no trivial loop, each disk face has at least two edges in its boundary. Each edge of Λ has two sides with distinct colors (black and white), because $\hat{T}$ is separating in S^3.

Now assume for a contradiction that there are only white faces. Then $E \geq 2F = 2E - 2d + 2$, and hence $E \leq 2d - 2$. This contradicts $E \geq 2d - 1$. It follows that there exists a black disk face. Similar argument shows that there exists a white disk face.

To prove the second part, suppose for a contradiction that each disk face of Λ has length at least four. Then we have $4F < 2E$. On the other hand, since $E \geq 2d-1$, we have $\frac{1}{2}E > F = E-d+1 \geq E-\frac{E+1}{2}+1 = \frac{E+1}{2}$, a contradiction. $\square$

In the following, a black (resp. white) Scharlemann disk is referred to as a black (resp. white) disk face.

Let H_{12} be the 1-handle $N(C)\cap V$ and H_{21} the 1-handle $\overline{N(C)\cap(S^3-V)}$; ∂V_1 and ∂V_2 give a partition of $\partial N(C)$ into two annuli $\overline{\partial H_{12} - \hat{T}}$ in the black side and $\overline{\partial H_{21} - \hat{T}}$ in the white side.

Let f be a disk face bounded by a Scharlemann cycle σ of G_D. Then the subgraph of G_T consisting of the two vertices V_1, V_2 and the corresponding edges of $\partial f = \sigma$ in G_T is called the *support* of f and denoted by f^*.

Lemma 3.4. *If f is a disk face in G_D, then its support f^* cannot be contained in a disk in $\hat{T}$.*

Proof. Assume that there exists a disk Z in $\hat{T}$ which contains the support f^*. Consider a regular neighborhood $M = N(Z \cup H \cup f)$ of $(Z \cup H \cup f)$, where H is H_{12} or H_{21} according to whether f lies in V or $S^3 - V$, respectively. Then M is a punctured (non-trivial) lens space in S^3, a contradiction (see [3] or [25] for more details). $\square$

Definition 3.5. Two edges in G_T are said to be *parallel*, if they cobound a disk in $\hat{T}$. Let $G_T(\Lambda)$ be the subgraph of G_T consisting of the two vertices V_1, V_2 and all the corresponding edges of Λ. Since all the vertices in Λ have the same sign, the edges in $G_T(\Lambda)$ join V_1 to V_2 by the parity rule [3]. Therefore there are at most four *edge classes* in G_T, i.e., isotopy classes of non-loop edges of G_T in $\hat{T}$ rel $\{V_1, V_2\}$, which we call $\alpha, \beta, \gamma, \theta$ as illustrated in Figure 6 (after some homeomorphism of $\hat{T}$). Representatives of distinct edge classes are not parallel.

Let $\mu \in \{\alpha, \beta, \gamma, \theta\}$. Such a label μ is referred to as the *edge class label* of e. An edge e in G_D (not necessarily in Λ) is called a *μ-edge* if the corresponding edge e in G_T belongs to μ-edge class.

Similarly, an edge e is said to be *a (μ, λ)-edge* if e is a μ-edge or a λ-edge, for two distinct edge class labels μ, λ. A cycle in G_D is called a *μ-cycle*, if it consists of only μ-edges.

Let f be a disk face of Λ. We define $\rho(f)$ to be the sequence (which is defined up to cyclic premutation) of edge class labels around ∂f, in the anti-clockwise direction, see Figure 7.

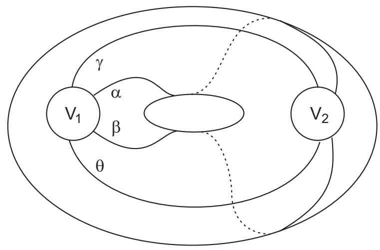

Figure 6

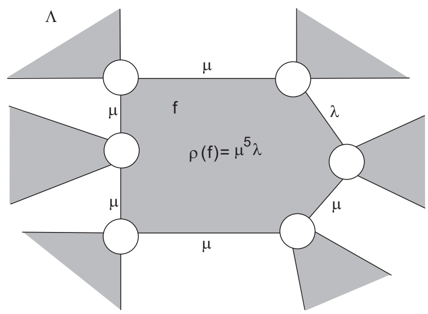

Figure 7

Let f be a disk face in G_D. If $\rho(f) = \mu^n$ for some edge class label $\mu \in \{\alpha, \beta, \gamma, \theta\}$, then the support f^* lies in a disk in $\hat{T}$, contradicting Lemma 3.4. We say that f is *primitive* if $\rho(f) = \mu^x\lambda$ (up to cyclic permutation) for some $\mu, \lambda \in \{\alpha, \beta, \gamma, \theta\}$ $(\mu \neq \lambda)$ and x a positive integer.

Lemma 3.6. *If f is a Scharlemann disk of length at most three, then f is primitive.*

Proof. This follows from [10, Lemma 3.7] and Lemma 3.4. □

We conclude this section with a sketch of the proof of Proposition 1.3.

Sketch of the proof of Proposition 1.3

Suppose that $K_n = K_{\Delta,n}$ is a satellite knot for some hyperbolic, twisting pair (K, Δ) and n with $|n| > 1$. We keep this assumption through Sections 4–7.

By Lemma 3.3 we have a disk face f of length at most three, which is primitive (Lemma 3.6) and hence its support is in an annulus in $\hat{T}$. The existence of such a disk face f assures the assumption of Propositions 3.7 or 3.8 below depending on whether f is black or white.

Proposition 3.7 (see Section 4 for its proof)**.** *If Λ contains a black face whose support lies in an annulus in $\widehat{T}$, then $K_{D,n}$ is a non-trivial cable of ℓ.*

Proposition 3.8 (see Section 5 for its proof)**.** *If Λ contains a white primitive face, then the companion knot ℓ is a non-trivial torus knot.*

To complete a proof of Proposition 1.3, we need another disk face g with the opposite colour of f. More precisely, if f is white, then we need g to be black whose support lies in an annulus in $\widehat{T}$; if f is black, then we need g to be white and primitive. This is given by the following two propositions.

Proposition 3.9 (see Section 6 for its proof)**.**
(*i*) *All black faces of Λ are isomorphic, i.e., if g, h are black faces of Λ then $\rho(g) = \rho(h)$;*
(*ii*) *If the disk face f is black, then Λ contains a white primitive face.*

Proposition 3.10 (see Section 5 for the proof of (i) and Section 7 for that of (ii))**.**
(*i*) *Λ cannot contain two white primitive faces with exactly one edge class label in common.*
(*ii*) *If the disk face f is white, then Λ contains a black face whose support lies in an annulus in $\widehat{T}$.*

Note that the proof of Proposition 1.3 in [12, Appendix A.2] is based on *good and binary faces*, which are disk faces with only two edge class labels, and such that one of them never appears successively twice around its boundary.

4. Topology of black disk faces supported by annuli

Recall that we have assumed that $K_n = K_{\Delta,n}$ is a satellite knot for some hyperbolic, twisting pair (K, Δ) and n with $|n| > 1$. The goal in this section is to prove Proposition 3.7

Let f_b be a black disk face with the support f_b^* in an annulus A in $\hat{T}$. Let $M_1 = N(A \cup H_{12} \cup f_b)$ be a regular neighbourhood of $A \cup H_{12} \cup f_b$. Push M_1 slightly inside V so that $M_1 \cap \partial V = A$; put $T_1 = \partial M_1$ and $B = T_1 - \mathrm{int}A$. Note that A is an essential annulus in $\hat{T}$ by Lemma 3.4. Put $A' = \hat{T} - \mathrm{int}A$, $T_2 = A' \cup B$, and let M_2 be a 3-manifold in V bounded by T_2, see Figure 8. Thus $V = M_1 \cup_B M_2$ and K_n lies in $\mathrm{int}M_2$.

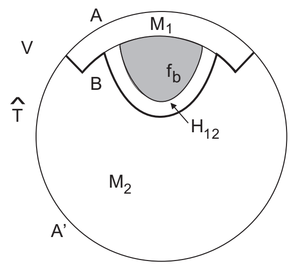

Figure 8

First we show that A is not a meridional annulus of V. Suppose that A is a meridional annulus (whose core bounds a meridian disk D_A), then we have the following two possibilities depending on whether $B \cap D_A = \emptyset$ or $B \cap D_A \neq \emptyset$, see Figure 9 below.

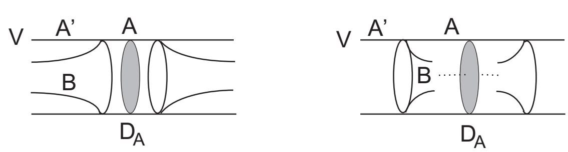

Figure 9

In the former case, K_n is contained in a 3-ball in V, a contradiction. So assume that the latter happens. Note that $T_2 \cap c_n = \emptyset$ and M_2 is a solid torus. Since M_2 is knotted in S^3 (because that V is knotted in S^3) and there is no 3-ball in $M_2(\subset V)$ containing K_n, T_2 is incompressible in $S^3 - \mathrm{int}N(K_n)$, and hence, in $S^3 - \mathrm{int}N(K_n \cup c_n)$. This then implies, together with the hyperbolicity of $S^3 - \mathrm{int}N(K_n \cup c)$, that T_2 is parallel to $\partial N(K_n)$, i.e., K_n is a core of M_2. If the annulus B is parallel to A, then it turns out that $\hat{T}$ is also parallel to $\partial N(K_n)$ contradicting the choice of V. Hence M_1 is a non-trivial knot exterior in a solid torus, as shown in Figure 10.

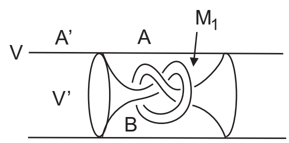

Figure 10

It follows that K_n is a composite knot. Then from [6, 13] we see that $|n| = 1$, contradicting the initial assumption.

Hence A is not a meridional annulus in V. Thus A is incompressible in V, and hence B ($\partial B = \partial A$) is also incompressible in V. This implies that B is a boundary-parallel annulus in V. If B is parallel to A, then M_2 (which is disjoint from c_n) is isotopic to V and T_2 is an essential torus in $S^3 - \mathrm{int}N(K_n)$, and hence in $S^3 - \mathrm{int}N(K_n \cup c_n)$, contradicting the hyperbolicity of $S^3 - \mathrm{int}N(K_n \cup c_n)$.

Therefore B is parallel to A'; B and A' cobounds the solid torus M_2 (which is disjoint from c_n).

Thus the core of M_2 is a cable of ℓ (a core of V). If T_2 is not parallel to $\partial N(K_n)$, then T_2 is an essential torus in $S^3 - \mathrm{int}N(K_n \cup c_n)$, contradicting the hyperbolicity of $S^3 - \mathrm{int}N(K_n \cup c_n) = S^3 - \mathrm{int}N(K \cup c)$. Hence T_2 is parallel to $\partial N(K_n)$, i.e., K_n is a core of M_2. It follows that K_n is a cable of ℓ (B wraps more than once in longitudinal direction of V).

5. **Topology of white primitive disk faces**

In this section we prove Proposition 3.8 and Proposition 3.10 (i).

5.1. **Proof of Proposition 3.8**

Let f_w be a white primitive disk face of Λ, satisfying $\rho(f_w) = \mu^x \lambda$ for two distinct edge class labels μ, λ and $x > 0$. Note that the support f_w^* lies in an essential annulus A_w in $\hat{T}$.

Let $M_{f_w} = N(A_w \cup H_{21} \cup f_w)$, which is a regular neighborhood of $A_w \cup H_{21} \cup f_w$ pushed slightly outside V, so that $T_3 = \partial M_{f_w} = A_w \cup B_w$, where B_W is an annulus properly embedded in $S^3 - \mathrm{int}V$ (see Figure 11).

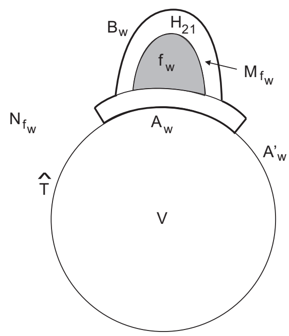

Figure 11

Put $A'_w = \hat{T} - \mathrm{int}A_w$, $T_4 = A'_w \cup B_w$. Denote by N_{f_w} the 3-manifold in $S^3 - \mathrm{int}V$ bounded by T_4; $S^3 - \mathrm{int}V = M_{f_w} \cup_{B_w} N_{f_w}$.

Claim 5.1. *M_{f_w} is a solid torus. Furthermore, the core of A_w wraps p times the core of the solid torus M_{f_w}, where $p = x + 1$.*

Proof. This was shown in [10, Lemma 3.7]. For convenience of readers, we give a proof here.

Note that $N(A_w) \cup H_{21}$ is a genus two handlebody and M_{f_w} is obtained from $N(A_w) \cup H_{21}$ by attaching a 2-handle $N(f_w)$. Let m_1 be a co-core of H_{21} intersecting ∂f_w p $(= x + 1)$ times in the same direction. Since $\sigma = \partial f_w$ has exactly one edge with the edge class label λ, we can choose a meridian disk m_2 of $N(A_w)$ intersecting ∂f_w once. Then m_1, m_2 form a set of meridional disks for the genus two handlebody $N(A_w) \cup H_{21}$. Since ∂f_w intersects m_2 once, ∂f_w is primitive and M_{f_w} is a solid torus. (This is the reason why we call f a primitive disk face.) Furthermore since the core of A_w intersects m_2 once and misses m_1, the core of A_w is homotopic to p times the core of the solid torus M_{f_w}. □

Claim 5.2. *N_{f_w} is a solid torus.*

Proof. Assume for a contradiction that N_{f_w} is not a solid torus. Then, by the solid torus theorem [24, p.107], $Y = S^3 - \mathrm{int}N_{f_w} = V \cup_{A_w} M_{f_w}$ is a (knotted) solid torus in S^3. Note that Y contains K_n and c_n in its interior. If there is a 3-ball in $Y = V \cup_{A_w} M_{f_w}$ containing K_n, then using the incompressibility of A_w in $S^3 - \mathrm{int}V$, we can find a 3-ball in V containing K_n, a contradiction. Thus ∂Y is incompressible in $S^3 - \mathrm{int}N(K_n)$, hence in $S^3 - \mathrm{int}N(K_n \cup c_n)$. Clearly ∂Y is not parallel to $\partial N(c_n)$. It follows from the hyperbolicity of $S^3 - \mathrm{int}N(K_n \cup c_n)$, ∂Y is parallel to $\partial N(K_n)$, i.e., K_n is a core of the solid torus Y.

Let D_Y be a meridian disk of $Y = V \cup_{A_w} M_{f_w}$ intersecting K_n exactly once. Assume further, by an isotopy, that D_Y intersects A_w transversely. Let D be a closure of a component of $D_Y - (D_Y \cap A_w)$ intersecting K_n. Then D is a meridian disk of V intersecting K_n exactly once. Since V is a knotted solid torus and K_n is not a core of V, K_n is a composite knot (of the form $\ell \sharp k$ for some non-trivial knot k, where ℓ is a core of V). Applying [6, 13], we can conclude that $|n| = 1$, contradicting the initial assumption. It follows that N_{f_w} is a solid torus. □

From Claims 5.1 and 5.2, we see that $S^3 - \mathrm{int}V$ is the union of two solid tori M_{f_w} and N_{f_w} such that $M_{f_w} \cap N_{f_w}$ is the annulus B_w. Since $A_w (= \partial M_{f_w} - \mathrm{int}B_w)$ wraps p times in the longitudinal direction of M_{f_w}, the annulus B_w wraps also p times in the longitudinal direction of M_{f_w}. If B_w is a meridian of N_{f_w}, then the knot exterior $S^3 - \mathrm{int}V = M_{f_w} \cup_{B_w} N_{f_w}$ contains a (non trivial) punctured lens space, a contradiction. Thus B_w wraps $q \geq 1$ times in longitudinal direction of N_{f_w}, and hence $S^3 - \mathrm{int}V = M_{f_w} \cup_{B_w} N_{f_w}$ is a Seifert fiber space over a disk with at most two exceptional fibers of indices $p \geq 2$ and q. Since V is knotted in S^3, $S^3 - \mathrm{int}V = M_{f_w} \cup_{B_w} N_{f_w}$ is not a solid torus. Hence $q \geq 2$ and ℓ (a core of V) is a non-trivial torus knot $T_{p,q}$ in S^3.

5.2. **Proof of Proposition 3.10 (i)**

Let us now prove Proposition 3.10 (i) in the following formulation.

Proposition 5.3. *Assume that Λ contains two white primitive disk faces f and g. Let $f_1, f_2, g_1, g_2 \in \{\alpha, \beta, \gamma, \theta\}$ such that $\rho(f) = f_1 f_2^m$ and $\rho(g) = g_1 g_2^n$, where m, n are positive integers. Then $\{f_1, f_2\} = \{g_1, g_2\}$ or $\{f_1, f_2\} \cap \{g_1, g_2\} = \emptyset$.*

Proof. We suppose for a contradiction that $\{f_1, f_2\} \cap \{g_1, g_2\} = \{\delta\}$, where $\delta = f_1$ or f_2. We repeat the construction and arguments in the proof of Proposition 3.8.

Let A_f, A_g be annuli in $\widehat{T}$ which contains the support of f and g, respectively. Let a_f, a_g be the cores of the annuli A_f, A_g, respectively. Then the minimal geometric intersection number between a_f and a_g is one: $|a_f \cap a_g| = 1$.

Let us recall the argument in Proposition 3.8; we use the analogous notations.
$M_f = N(A_f \cup H_{21} \cup f)$,
$B_f = \partial M_f - \mathrm{int} A_f$,
$N_f = S^3 - \mathrm{int}(V \cup M_f) \subset S^3 - \mathrm{int} V$,
$A'_f = \partial N_f - \mathrm{int} B_f$.
So $\widehat{T} = A_f \cup A'_f$ and $S^3 - \mathrm{int} V = M_f \cup_{B_f} N_f$.

By the proof of Proposition 3.8, M_f, N_f are solid tori and $S^3 - \mathrm{int} V$ is a Seifert fiber space over a disk with two exceptional fibers which are the core of M_f and N_f. The annulus B_f is essential in $S^3 - \mathrm{int} V$. We repeat the analogous construction of Proposition 3.8 for the white disk face g:
$M_g = N(A_g \cup H_{21} \cup g)$,
$N_g = S^3 - \mathrm{int}(V \cup M_g) \subset S^3 - \mathrm{int} V$,
$B_g = \partial M_g - \mathrm{int} A_g$, and $A'_g = \widehat{T} - A_g$. Then $S^3 - \mathrm{int} V = M_g \cup_{B_g} N_g$.

In the same way as for f (see the proof of Proposition 3.8) we show that N_g and M_g are solid tori and B_g is an essential annulus properly embedded in $S^3 - \mathrm{int} V$.

Then B_g is isotopic to B_f in $S^3 - \mathrm{int} V$, because that $S^3 - \mathrm{int} V$ is a Seifert fiber space over a disk with two exceptional fibers and any essential annulus is isotopic to B_f. Hence a component of ∂B_f (which is isotopic to a_f on $\hat{T}$) and a component of ∂B_g (which is isotopic to a_g on $\hat{T}$) are isotopic on $\widehat{T}$, contradicting $|a_f \cap a_g| = 1$. $\square$

6. **Existence of white primitive disk faces**

This section is devoted to prove Proposition 3.9.

6.1. **Proof of Proposition 3.9 (i)**

Put $M = V - \mathrm{int}N(K_n)$ and $W = \overline{M - H_{12}}$. Then ∂W has two boundary components: $\partial W_+ = T \cup (\partial H_{12} - \hat{T})$, which is a surface of genus two, and $\partial W_- = \partial N(K_n)$.

Let f_b be a black disk face of Λ bounded by a Scharlemann cycle σ_b. Since all the vertices of σ_b have the same sign, ∂f_b is a non-separating (essential) simple closed curve on ∂W_+. Consider $Z = N(\hat{T} \cup H_{12} \cup f_b) \subset M$. Then ∂Z has two tori $\hat{T}$ and T_Z. Let V' be the 3-manifold in V bounded by T_Z, which contains K_n in its interior.

Claim 6.1. *T_Z is parallel to $\partial N(K_n)$.*

Proof. If T_Z is compressible in $V' - \mathrm{int}N(K_n)$, then there would be a 3-ball in $V' \subset V$ containing K_n, a contradiction. If T_Z is compressible in $S^3 - \mathrm{int}V'$, then $S^3 - \mathrm{int}V'$ is a solid torus. Since $\hat{T}$ is incompressible in $S^3 - \mathrm{int}N(K_n)$, it is also incompressible in the solid torus $S^3 - \mathrm{int}V'$, a contradiction. Therefore T_Z is incompressible in $S^3 - \mathrm{int}N(K_n)$, hence in $S^3 - \mathrm{int}N(K_n \cup c_n)$ and T_Z is not parallel to $\partial N(c_n)$. The initial assumption of the hyperbolicity of $S^3 - \mathrm{int}N(K_n \cup c_n) \cong S^3 - \mathrm{int}N(K \cup c)$ implies that T_Z is parallel to $\partial N(K_n)$. $\square$

From Claim 6.1, we see that W can be regarded as a manifold obtained from $\partial N(K_n) \times [0, 1]$ by attaching $N(f_b)$ as a 1-handle (i.e., W is a compression body). Then f_b is the unique non-separating disk in W, up to isotopy.

Now we follow the argument in [11, Lemma 5.6] to show that all the black disk faces of Λ are isomorphic. Let g_b be another black disk face of Λ. Since f_b and g_b are isotopic in W, ∂f_b and ∂g_b are isotopic in ∂W_+, and hence freely homotopic in $\hat{T} \cup H_{12}$.

We re-label edge class labels by $\gamma = 1$, $\theta = \alpha\beta$. Then $\pi_1(\hat{T} \cup H_{12}) \cong \pi_1(\hat{T}) * \mathbb{Z}$, where, taking as base-“point" a disk neighborhood in $\hat{T}$ of an edge in G_T in edge class 1, $\pi_1(\hat{T}) \cong \mathbb{Z} \times \mathbb{Z}$ has basis $\{\alpha, \beta\}$, represented by edges in the correspondingly named edge classes, oriented from V_2 to V_1, and $\mathbb{Z}$ is generated by x represented by an arc in H_{12} going from V_1 to V_2.

Then if $\rho(f_b) = \gamma_1 \cdots \gamma_m$, then ∂f_b represents $\gamma_1 x \gamma_2 x \cdots \gamma_m x \in \pi_1(\hat{T}) * \mathbb{Z}$. Similarly if $\rho(g_b) = \lambda_1 \cdots \lambda_n$, then ∂g_b represents $\lambda_1 x \lambda_2 x \cdots \lambda_n x \in \pi_1(\hat{T}) * \mathbb{Z}$. Since ∂f_b and ∂g_b are homotopic in $\hat{T} \cup H_{12}$, we conclude that the corresponding sequences $\gamma_1 \cdots \gamma_n$ and $\lambda_1 \cdots \lambda_m$ are equal, up to cyclic permutation, i.e., f_b and g_b are isomorphic.

6.2. **Proof of Proposition 3.9 (ii)**

A disk face of length two or three is called a *bigon* or a *trigon*, respectively. Assume that the disk face f given by Lemma 3.3 is black, which has length at most three. Then, by Proposition 3.9 (i), all the black disk faces of Λ are isomorphic bigons or isomorphic trigons. Furthermore, they are primitive by Lemma 3.6.

We begin by observing the following:

Claim 6.2. *Let v be a vertex of Λ and e, e' edges of Λ incident to v with the same label. Then e and e' have distinct edge class labels.*

Proof. This follows from [11, Lemma 5.3]. If e and e' have the same edge class label, then they would be parallel in G_T, and hence would cobound a family of $q+1$ parallel edges of G_T. This then implies that $M = S^3 - \mathrm{int}N(K \cup c)$ contains a cable space ([8, p.130, Case(2)]), contradicting the hyperbolicity of M. □

Now assume that two isomorphic black bigons (resp. trigons) g_1 and g_2 of Λ, with $\rho(g_i) = \mu\lambda$ (resp. $\rho(g_i) = \mu^2\lambda$) are incident to a same vertex v of Λ. Then by Claim 6.2 the labels of the edges incident to v are $\lambda, \mu, \mu, \lambda$ in cyclic order around v as in Figure 12 below. We call this a *property* $(*)$.

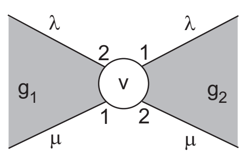

Figure 12

The proof of Proposition 3.9 is divided into two cases depending on whether the black disk faces are bigons or trigons.

Lemma 6.3. *If all the black disk faces of Λ are isomorphic bigons, then there exists a white primitive disk face.*

Proof. Assume that for each black bigon g, we have $\rho(g) = \mu\lambda$, for some edge class labels $\mu, \lambda \in \{\alpha, \beta, \gamma, \theta\}$ ($\mu \neq \lambda$). There are three cases to consider: Λ has

(1) no vertex with ghost labels,
(2) exactly one vertex with ghost labels, and
(3) two vertices with ghost labels.

Case (1): Λ has no vertex with ghost labels.
If the annulus face f_0 is white, then Λ has a unique white face f surrounded by black bigons. By the property $(*)$ all the edges of ∂f have the same label, say μ, see Figure 13.

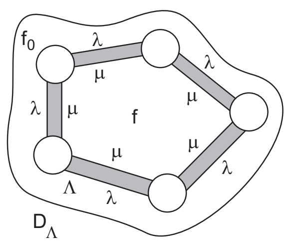

Figure 13

Then the support f^* of the white Scharlemann disk f lies in a disk, contradicting Lemma 3.4.

Hence f_0 is black. Let v_0 be a boundary vertex of Λ. Then there is a black bigon b_0, which joins v_0 to another vertex v_1. If v_1 is an interior vertex, then since the valence of v_1 is four, v_1 is incident to another black bigon b_1. Repeating this until we arrive at a boundary vertex, we obtain a sequence of black bigons $b_0, b_1, \ldots, b_n$ such that b_i and b_{i+1} are incident to the same interior vertices; see Figure 14. The sequences of black bigons obtained in this manner (for all the boundary vertices) give a partition of the disk bounded by boundary edges of Λ into several white disk faces. Let f be an outermost white disk face (which has only one boundary edge). From property $(*)$, we see that $\rho(f) = \mu^n\delta$ or $\rho(f) = \lambda^n\delta$, for some $\delta \in \{\alpha, \beta, \gamma, \theta\}$; (note that the boundary vertex v_0 may not satisfy the property $(*)$). Thus f is a required white primitive disk face.

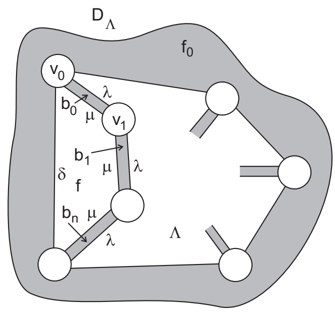

Figure 14

Case (2): Λ has a unique vertex v_0 with ghost edges.
Since each vertex of Λ except for v_0 has valence four and the number of edge endpoints of Λ is even, v_0 has two ghost labels.

Let $\Lambda' \subset D_\Lambda$ be a graph obtained from Λ by connecting two arcs incident to v_0 with ghost labels as shown in Figure 15; the additional edge obtained in such a manner is called an *extra edge*. Then the annulus face f_0 is replaced by two faces: a disk face f_0^- and an annulus face f_0^+ with distinct colors. Then f_0^+ contains all the boundary edges, see Figure 15.

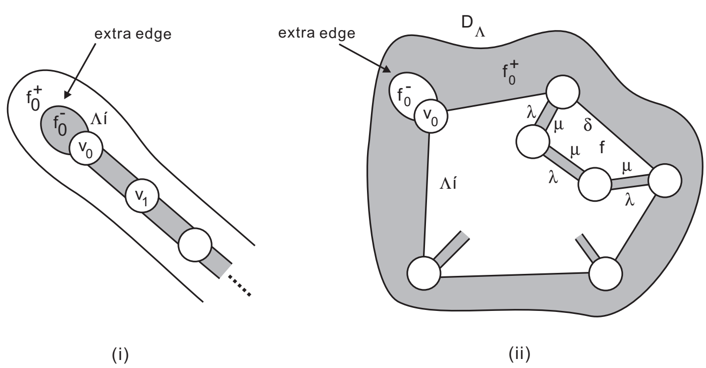

Figure 15

If f_0^- is black, then v_0 is incident to a black bigon b_0 of of Λ, which is incident to another vertex v_1. Since v_1 has valence four and has no ghost labels, we have another black bigon incident to v_1. By repeating this, we obtain an infinite sequence of black bigons, contradicting the finiteness of the graph Λ, see Figure 15 (i). Thus f_0^+ is black. Applying the same argument in Case (1), we can find a required white primitive disk face f as in Figure 15 (ii).

Case (3): Λ has two vertices v_1 and v_2 each of which has a ghost label. As in Case (2) we consider a graph $\Lambda' \subset D_\Lambda$ which is obtained from Λ by connecting two arcs incident to v_i $(i = 1, 2)$ with ghost labels, see Figure 16.

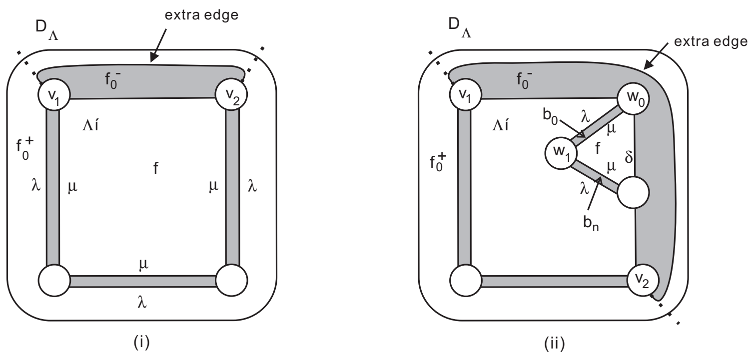

Figure 16

The annulus face f_0 is replaced by a disk face f_0^- and an annulus face f_0^+ with distinct colors; the boundary vertices v_1 and v_2 are contained in their boundaries.

First we assume that the disk face f_0^- is black (as in Figure 16). Then since f_0^+ is white, every edge in ∂f_0^+ other than the extra edge is an edge of a black bigon of Λ.

If ∂f_0^- has only two vertices v_1 and v_2, then Λ has a unique white disk face surrounded by black bigons; except f_0^- each bigon is a bigon in Λ, Figure 16 (i). By property $(*)$, the white disk face is primitive, see the argument in Case (1).

So we assume that ∂f_0^- contains a vertex w_0 other than v_1, v_2 as shown in Figure 16 (ii). Then there is a black bigon b_0 incident to w_0. We follow the argument in Case (1). The black bigon b_0 connects w_0 and another vertex w_1. Note that w_1 is not in ∂f_0^+, because each vertex in ∂f_0^+ has been already incident to two bigons each of which has an edge in ∂f_0^+. If w_1 is interior vertex, then we have a black bigon connecting w_1 and another vertex, and repeating this, we obtain a sequence of black bigons $b_0, b_1, \dots, b_n$ such that b_i and b_{i+1} are incident to the same interior vertex and that b_0 and b_n are incident to distinct boundary vertices in ∂f_0^-. These sequences give a partition of the disk bounded by boundary edges of Λ into several white disk faces. Let f be an outermost white disk face (which has only one boundary edge in ∂f_0^-). By the property $(*)$, $\rho(f) = \mu^n\delta$ or $\rho(f) = \lambda^n\delta$, for some $\delta \in \{\alpha, \beta, \gamma, \theta\}$, see Figure 16 (ii). Thus f is a required white primitive disk face.

Next suppose that the disk face f_0^- is white (i.e., f_0^+ is black). If ∂f_0^+ has exactly two vertices, then we have a required white primitive disk face f as in Figure 17 (i) below. Assume that ∂f_0^+ has more than two vertices. Choose a vertex w_0 in ∂f_0^+ which is not in ∂f_0^-. Then we apply the same argument as above (w_1 may be in ∂f_0^+) to find a required white primitive disk face f, see Figure 17 (ii).

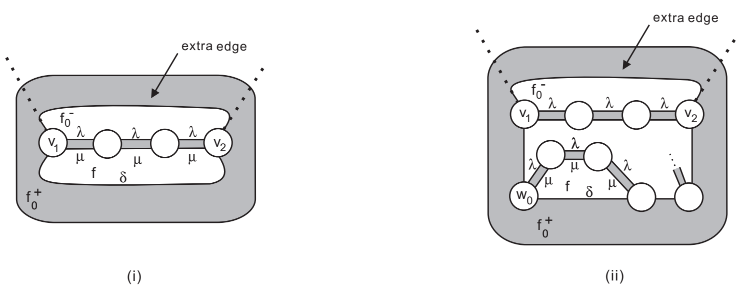

Figure 17

□

Lemma 6.4. *If all the black disk faces of Λ are isomorphic trigons, then there exists a white primitive disk face.*

Proof. By Lemma 3.6, we can assume that for each black trigon g of Λ, $\rho(g) = \mu^2\lambda$ for some $\mu, \lambda \in \{\alpha, \beta, \gamma, \theta\}$.

We start with the following observation:

Claim 6.5. *Let g be a black trigon of Λ. Then at most two vertices of g can be incident to black trigons of Λ.*

Proof. Assume for a contradiction that a black disk face g is incident to three black trigons. Without loss of generality, the edge class labels appear around g as in Figure 18.

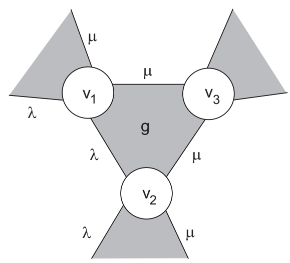

Figure 18

Then at least one vertex, say v_3 in Figure 18, fails to satisfy the property $(*)$, a contradiction. □

Let us first assume that Λ has more than four boundary vertices. The interior edges of Λ decompose the disk bounded by Λ into several disk faces.

Claim 6.6. *There exists an outermost disk face f which has a single boundary edge e of Λ connecting two boundary vertices x and y to none of which ghost edges are incident.*

Proof. Assume that $\Lambda - \{\text{boundary edges}\}$ is connected; then each outermost disk face of Λ has only single boundary edge. Since the number of outermost disk faces, which coincides with the number of boundary vertices, is greater than four, we can find a required outermost disk face. Next suppose that $\Lambda - \{\text{boundary edges}\}$ is not connected. If some component Λ' of $\Lambda - \{\text{boundary edges}\}$ has a single boundary vertex v, then Λ' consists of the single vertex v and two ghost labels (without edges of Λ). Because if v has no ghost edges, then the component is also a great web, contradicting the minimality of Λ (Figure 19 (i)); if v has only one ghost edge, then the both (local) sides of the edge e incident to v have the same color as shown in Figure 19 (ii), a contradiction.

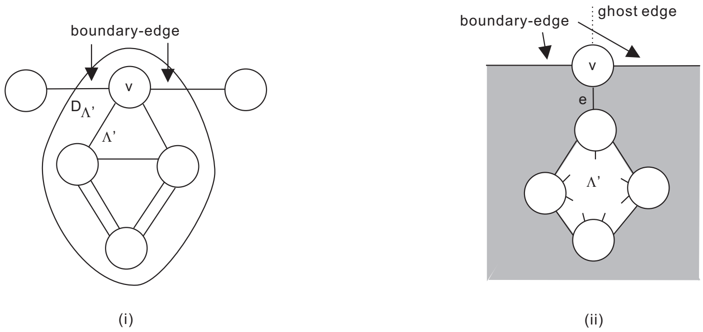

Figure 19

Case (1): There is a component with a single boundary vertex.
Then this vertex has two ghost labels as above. Let Λ_0 be any other component, which has at least two boundary vertices and none of which has ghost labels. Then an outermost disk face cut off by Λ_0 is the required disk face.

Case (2): There is no component with a single boundary vertex.
Then each component has at least two boundary vertices. If we have more than two components, then since there are at most two ghost edges, some component has no ghost edges, which cuts off a required disk face. If we have exactly two components, since we have at most two ghost edges, there are two possibilities: each component has a ghost edge, or exactly one of them has two ghost edges. In the former case, there would exsist an edge whose both sides have the same color (Figure 20 (i)), a contradiction. In the latter case, let Λ_0 be a component having no ghost edges (Figure 20 (ii)). Then as above Λ_0 cuts off a required disk face. $\square$

Let us choose an outermost disk face f with a single boundary edge e as in Claim 6.6. Suppose that f is a black disk face with the third vertex z. If the vertex z is an interior vertex, then f is incident to three trigons at x, y and z, contradicting Claim 6.5. Thus z is also a boundary vertex. Since x (resp. y) has no ghost edges and it has valence four, we can take another black trigon f_x (resp. f_y) incident to x (resp. y); denote the other two vertices of f_x by v, w, see Figure 21. We choose v so that the edge in f_x connecting x and v is an interior edge of Λ. Since both vertices x and

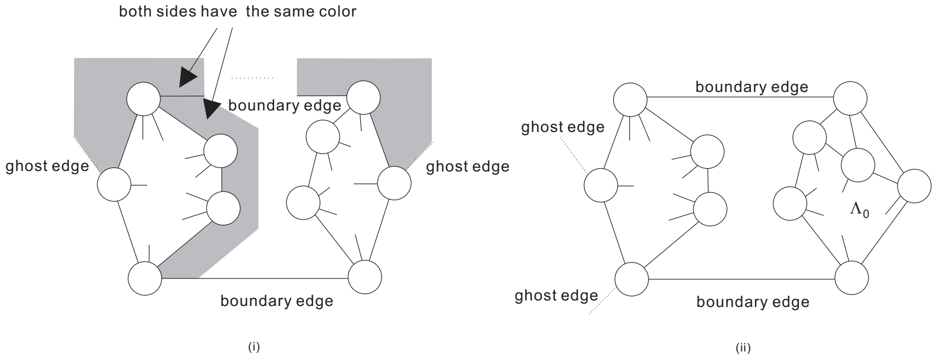

FIGURE 20

y satisfy the property $(*)$, e has the edge class label λ and two edges of f_x incident to x have distinct edge class label μ, λ as in Figure 21. This then implies that the edges of f_x incident to v both have the same edge class label μ (because $\rho(f_x) = \mu^2\lambda$). Thus v cannot satisfy the property $(*)$ and hence it is a boundary vertex of Λ. If there is no boundary vertex between z and v, then three vertices x, z and v determines a white trigon, which is primitive, see Figure 21.

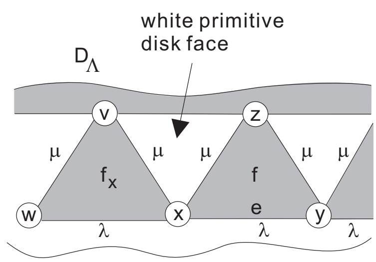

FIGURE 21

Let us suppose that there is another boundary vertex between z and v, see Figure 22. By Claim 6.5, each black trigon contains a boundary vertex. This then implies that there is a white bigon or trigon (Figure 22), which is primitive by Lemma 3.6.

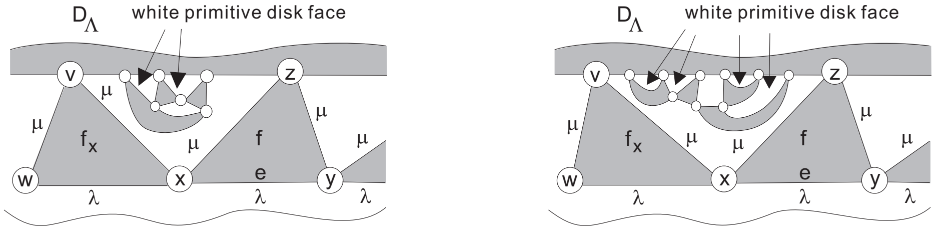

FIGURE 22

Suppose that f is a white disk face. Then by the property $(*)$ all the edges of f, except for the boundary edge e, have the same label μ or λ. Thus f is a required white primitive disk face, see Figure 23.

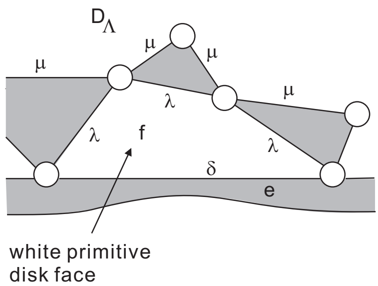

FIGURE 23

It follows that if Λ has more than four boundary vertices, there is a desired white primitive disk face.

If the number of boundary vertices of Λ is less than four, then it is not difficult to show that we can find a required white primitive disk face or there would be a black trigon whose three vertices are incident to black trigons, contradicting Claim 6.5.

Assume that Λ has exactly four boundary vertices. If there is a boundary edge incident to two vertices without ghost labels (Figure 24 (i)), then we consider the disk face f, which contains the boundary edge e as in Figure 24 (i).

We apply the previous argument to show that Λ contains a white primitive disk face as desired. So we may suppose that each boundary edge has a vertex with a ghost label as in Figure 24 (ii). Then up to symmetry Λ has a form described in Figure 24 (ii), because each black trigon is incident to at most two black trigons (Claim 6.5).

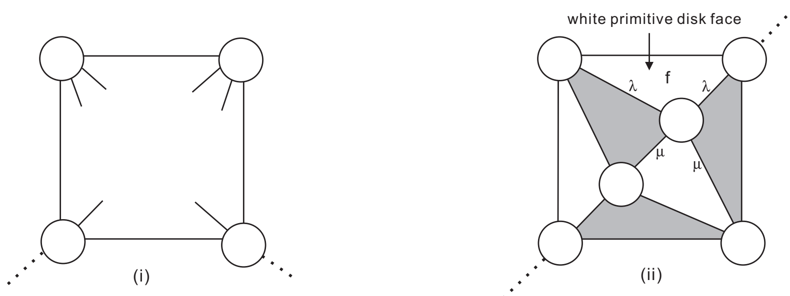

FIGURE 24

So we have a required white primitive disk face f as in Figure 24 (ii). This completes a proof of Lemma 6.4. □

7. Existence of black disk faces supported by annuli

This section is devoted to a proof of Proposition 3.10 (ii). Notice that the arguments are close to those in [12].

Assume that the disk face f given by Lemme 3.3 is white, which has length ≤ 3. Then by Lemma 3.6, we assume throughout this section (if necessary changing the edge class labels) that $\rho(f) = \alpha^n\beta$ with $n = 1$ or 2.

Claim 7.1. *Let g be a primitive disk face of Λ with $\rho(g) = \mu^m\lambda$ for some $\mu, \lambda \in \{\alpha, \beta, \gamma, \theta\}$ such that $\{\mu, \lambda\} \neq \{\alpha, \beta\}$ and $\{\mu, \lambda\} \cap \{\alpha, \beta\} \neq \emptyset$, e.g. $\{\mu, \lambda\} = \{\alpha, \gamma\}$. Then g is a black disk face whose support is lying in an annulus in $\hat{T}$.*

Proof. Proposition 3.10 (i) shows that g cannot be white, i.e., g is black. Since g is primitive, its support lies in an annulus in $\hat{T}$. □

In the following, we assume, if necessary changing the notations γ, θ, that the γ-family (i.e., the set of γ-edges) is adjacent to the α-family around ∂V_1 (Figure 6). Consequently, the θ-family is adjacent to the β-family.

7.1. **Oriented dual graphs**

Let us construct an *oriented dual graph* Γ ([10, p. 633]), which has an essential role in the proof of Proposition 3.10. For each face f of Λ, choose a *dual vertex* v so that $v \in \mathrm{int} f$. Each edge e of Λ has two sides, i.e., black side and white side, each of which has a unique dual vertex. An edge ε of Γ is an edge transverse to e which joins the above two dual vertices. We call ε a *dual edge* of e and e an *associated edge* of ε. Finally we put an orientation on each edge of Γ according to the following rule: For each edge ε of Γ which is a dual edge of e with edge class label $\delta \in \{\alpha, \beta, \gamma, \theta\}$, we fix an orientation WB or BW, say as indicated in Figure 25.

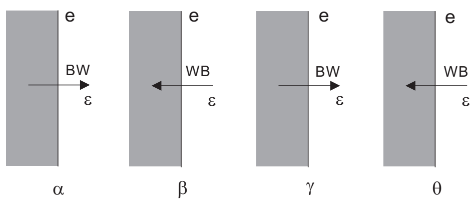

Figure 25

For later convenience, we say that an edge e of Λ is a *BW-edge* (resp. *WB-edge*) if its dual edge ε of Γ has an orientation BW (resp. WB). Let us denote the dual graph with dual orientation defined in Figure 25 by $\Gamma^{\alpha,\gamma}_{\beta,\theta}$. Similarly if the dual orientation is chosen as indicated in Figure 26, then the dual graph with such a dual orientation is denoted by $\Gamma^{\alpha}_{\beta,\gamma,\theta}$.

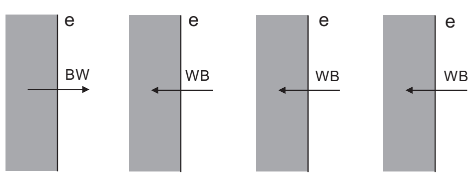

Figure 26

For each vertex v of Γ, let $s(v)$ be the number of switches (i.e., changes in orientation of successive edges) around v, and for each face f of Γ, let

$s(f)$ be the number of switches (i.e., same orientation of successive edges) around ∂f; see Figure 27.

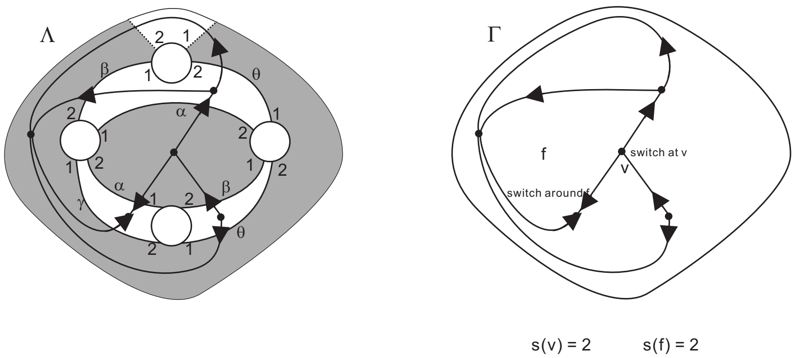

Figure 27

Define the *index* of a vertex v or face f by

$$I(v) = \chi(f_v) - \frac{s(v)}{2},\ I(f) = 1 - \frac{s(f)}{2},$$

where f_v denotes the face of Λ containing the dual vertex v. We say that a vertex v of Γ is *a positive vertex* if $I(v) > 0$. We say that a face f of Γ is *a cycle-face* if $I(f) > 0$. (By definition $I(f) \leq 1$, so f is a cycle face if and only if $I(f) = 1$.) A fat vertex X of Λ is *a cycle-vertex* if the corresponding face of Γ is a cycle-face, see Figure 28.

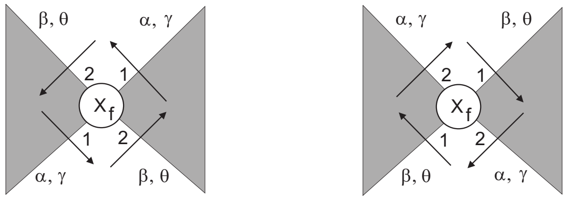

Figure 28

In the following, we say that an edge of Λ is an (α,γ)-*edge* (resp. a (β,θ)-*edge*) if it is an α-edge or a γ-edge (resp. a β-edge or a θ-edge). Similarly an edge e of Λ is said to be a (β,γ,θ)-*edge* if e is not an α-edge.

Let us denote $\partial_\Lambda f_0 = \partial f_0 \cap \Lambda$; recall that f_0 is the single annulus-face of Λ. After fixing an oriented dual graph Γ, we say that a cycle of Λ is a BW-*cycle* (resp. WB-*cycle*) if it consists of BW-edges (resp. WB-edges).

Lemma 7.2. *Let Γ be an oriented dual graph such that the BW-edges (resp. WB-edges) of Λ are adjacent families around ∂V_1.*

Assume that Γ does not contain a positive vertex, then we have the following:

(1) *Λ has exactly two cycle-vertices X_1 and X_2. Furthermore, both of them have one ghost label.*

(2) *$\partial_\Lambda f_0$ is a BW-cycle (resp. WB-cycle) and both X_1, X_2 are incident to an interior WB-edge (resp. BW-edge).*

(3) *For each disk face h of Λ, there exist positive integers m, n such that*

$$\rho(h) = \delta_1^1\delta_1^2 \dots \delta_1^m \delta_2^1\delta_2^2 \dots \delta_2^n \ (\textit{up to cyclic permutation}),$$

where the δ_1^i's are BW-edges and the δ_2^j's are WB-edges.

(4) *$\partial_\Lambda f_0$ is not a δ-cycle, for $\delta \in \{\alpha,\beta,\gamma,\theta\}$.*

Proof. Following [4] or [9] we have:

Claim 7.3. $\sum I(v) + \sum I(f) = 1$ *(summed over all vertices v and all faces f of Γ).*

Proof. Recall that all faces of Λ in D_Λ, except the outermost annulus face f_0, are disk faces, and that d (the number of vertices of Λ) coincides with the number of faces of Γ.

Let V, E be the number of vertices, edges of Γ, respectively.

Then we have:

(1) $\sum I(v) = \sum \chi(f_v) - \sum \frac{s(v)}{2} = (V-1) - \sum \frac{s(v)}{2}$, and

(2) $\sum I(f) = d - \sum \frac{s(f)}{2} = \sum \chi(f) + 1 - \sum \frac{s(f)}{2}$.

Each corner between adjacent edges at a vertex contributes exactly 1 to $\sum s(v)+\sum s(f)$, the Euler formula, together with (1), (2), gives

$$\begin{aligned}
1 &= V-E+\sum\chi(f)\\
&= V-\frac{\textit{the number of corners}}{2}+\sum\chi(f)\\
&= V-\frac{\sum s(v)+\sum s(f)}{2}+\sum\chi(f)\\
&= \sum I(v)+\sum I(f).
\end{aligned}$$

□

Assume that there is no positive vertex of Γ.

(1) By Claim 7.3, there exists a cycle-face f in Λ. We denote by X an associated cycle-vertex, and x the corresponding label in G_T.

Claim 7.4. *A cycle-vertex X cannot have valence four.*

Proof. Assume for a contradiction that X has valence four. Then the edges around ∂X incident to the label 1 are BW-edges (resp. WB-edges) and the edges around ∂X incident to the label 2 are WB-edges (resp. BW-edges), see Figure 28.

Without loss of generality, we may assume that the BW-edges have label 1 at ∂X; and that the WB-edges have label 2 at ∂X. Thus ∂V_1 contains the label x twice at the adjacent families of BW-edges; and similarly, ∂V_2 contains the label x twice at the adjacent families of WB-edges.

If Λ has no ghost edge, then there are at least $d+1$ BW-edges of $G_T(\Lambda)$ and the same is true for the WB-edges. On the other hand, there are only $2d$ edges in Λ, a contradiction.

If Λ has ghost edges, then there are two possibilities: we have a boundary vertex incident to two ghost edges, or we have two boundary vertices each of which has a single ghost edge (see the proof of Lemma 6.3). In either case, ghost labels are distinct and there are at least d BW-edges and d WB-edges. However there are only $2d-1$ edges in Λ, a contradiction. □

Let v_0 be the dual vertex which corresponds to the annulus face f_0 of Λ. Then $I(v_0)=-s(v_0)/2$. By Claim 7.4 the valence of X is two or three, in particular, X is a boundary vertex (with ghost edges). Therefore, there is a switch at v_0 and thus $I(v_0)\le -1$, see Figure 29. Consequently $I(f)+I(v_0)\le 0$. Thus by Claim 7.3 there is another cycle-face. Since Λ has at most two ghost edges, by Claim 7.4 there are exactly two cycle-vertices, and both of them have valence three.

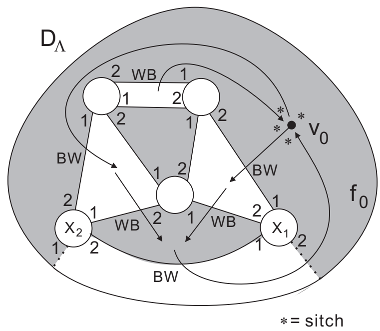

Figure 29

(2) Let us denote X_1, X_2 the two cycle-vertices, and x_1, x_2 their corresponding labels in G_T. Without loss of generality, we may assume that the ghost label at X_1 is 2. Then the two edges of Λ incident to X_1 at the label 1 are BW-edges or both of them are WB-edges; we may assume that these edges are BW-edges. Note that if there is a WB-edge in $\partial_\Lambda f_0$, then $s(v_0) \geq 4$ and so $I(v_0) \leq -2$, see Figure 30. By Claim 7.3,

$$\sum_{v \neq v_0} I(v) + \sum_{f \neq f_1, f_2} I(f) \geq 1.$$

This then implies that there is a face with positive index, i.e., cycle-vertex other than X_1, X_2, contradicting (1). It follows that all the edges in $\partial_\Lambda f_0$ are BW-edges. Furthermore, the interior edges incident to X_1 and X_2 are WB-edges, since they are cycle-vertices.

(3) Let h be a disk face of Λ. It is sufficient to observe that, up to cyclic permutation, all the BW-edges are successive. Assume not, then there are at least four switches at v_h and $I(v_h) < -1$, where v_h is the dual vertex of h. Furthermore, from (1) we see that v_0 has at least two switches and $I(v_0) \leq -1$. Since we have assumed that there is no positive vertex, $I(v) \leq 0$ for $v \neq v_0, v_h$. Hence Claim 7.3 shows that

$$\sum I(f) \geq 1 - (I(v_0) + I(v_h) + \sum_{v \neq v_0, v_h} I(v)) \geq 3.$$

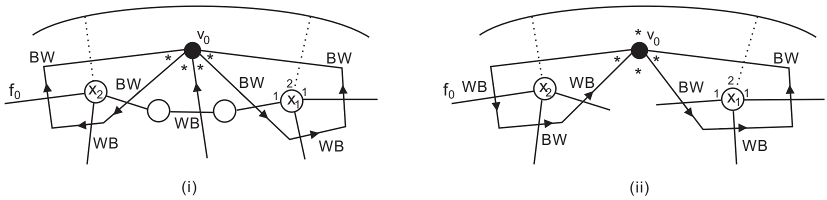

Figure 30

This is impossible, because that only X_1, X_2 are cycle-vertex (by (1)) and $\sum I(f) \leq 2$.

(4) Let $\delta \in \{\alpha, \beta, \gamma, \theta\}$. If $\partial_\Lambda f_0$ is a δ-cycle, then there would be two δ-edges incident to X_1 at label 1 (or 2), contradicting Claim 6.2. $\square$

Let h be a disk face of Λ and δ_1, δ_2 in $\{\alpha, \beta, \gamma, \theta\}$. The boundary of h is an alternative sequence of edges of Λ and *corners*. Let C be a corner on ∂h. Then C is an arc on the boundary of a fat vertex X of Λ; we say that C is an X-*corner*. Furthermore, we say that C is a $< \delta_1, \delta_2 >$-*corner* if the edge incident to C with label 1 (resp. 2) has edge class label δ_1 (resp. δ_2), see Figure 31.

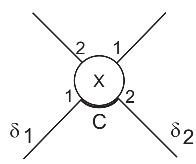

Figure 31

When $\delta_1 = \delta_2 = \delta$, we say simply that C is a $< \delta >$-*corner*. Note that ∂h has a $< \delta >$-corner if and only if there are two successive δ-edges on ∂h.

Recall that f is a white disk face of Λ such that $\rho(f) = \alpha^n \beta$ ($n = 1$ or 2). Thus there are an $< \alpha, \beta >$-corner and a $< \beta, \alpha >$-corner : see Figure 32, where the α-family is adjacent to the β-family around ∂V_1. Notice that in such a figure, the edges are corners; in this one they are (α, β)-corners. Note that if we put edge class labels as in Figure 6, then for an orientation of ∂V_1 and ∂V_2, edges class labels appear in cyclic order $\alpha, \beta, \theta, \gamma$ around ∂V_1 and $\alpha, \gamma, \theta, \beta$ around ∂V_2.

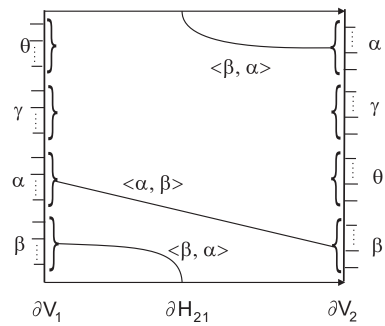

Figure 32

We divide the proof of Propositions 3.10 (ii) into two cases according to whether the θ-family and the γ-family are non-empty (Case 1) or at least one of them is empty (Case 2).

7.2. Proof of Proposition 3.10 (ii)–Case 1

In this subsection, we assume that: *The γ-family and the θ-family are non-empty.*

Recall that $\Gamma^{\alpha,\gamma}_{\beta,\theta}$ is the oriented dual graph, for which α, γ are BW-edges and β, θ are WB-edges.

Lemma 7.5. *If there is no black disk face whose the support lies in an annulus in $\widehat{T}$, then there exists a positive vertex in $\Gamma^{\alpha,\gamma}_{\beta,\theta}$.*

Proof. Assume for a contradiction that $\Gamma^{\alpha,\gamma}_{\beta,\theta}$ does not have a positive vertex. Then applying Lemma 7.2, we see that $\partial_\Lambda f_0$ is a BW-cycle (i.e., a (α, γ)-cycle) or a WB-cycle (i.e., a (β, θ)-cycle). Whithout loss of generality, we may assume that $\partial_\Lambda f_0$ is a (α, γ)-cycle.

Claim 7.6. *All the vertices of Λ, except for X_1 and X_2, are incident to (α, γ)-edges with both labels* 1 *and* 2*.*

Proof. There is a sequence of edges (i.e., a subgraph homeomorphic to a simple arc when vertices are considered as points) in $\partial_\Lambda f_0$ that joins the cycle vertices X_1 and X_2; we assume that the ghost label at X_1 is 2 and that of X_2 is 1. Then the two edges of Λ incident to X_1 (resp. X_2) at the label 1 (resp. 2) are both (α, γ)-edges. Thus, in $G_T(\Lambda)$, the vertex V_1 has two labels x_1 at endpoints of (α, γ)-edges; and simlilarly, the vertex V_2 has two labels x_2 at endpoints of (α, γ)-edges. Therefore all the vertices of Λ, except for X_1 and X_2, are incident to (α, γ)-edges with both labels 1 and 2. □

Let us choose an (α, γ)-cycle τ as follows. If there is no interior (α, γ)-edge, then τ is $\partial_\Lambda f_0$. If there are interior (α, γ)-edges, then τ is the union of a sequence of (successive) boundary (α, γ)-edges $e_1, \ldots, e_m$ connecting boundary vertices Y_1 and Y_2 and a sequence of (successive) interior (α, γ)-edges $\varepsilon_1, \ldots, \varepsilon_n$ connecting Y_1 and Y_2; the sequence of interior edges is *oriented* in the sense that for some orientation of the sequence, each edge in the sequence is oriented from the label 1 to the label 2, see Figure 33. A cycle is said to be *oriented* if for some orientation of the cycle, each edge in the cycle is oriented from the label 1 to the label 2.

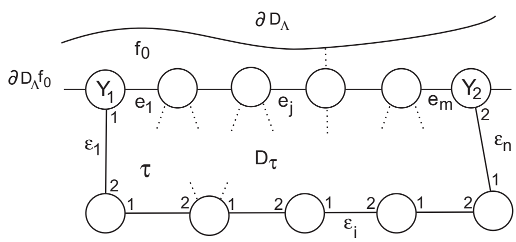

Figure 33

Claim 7.7. *If* $\Gamma^{\alpha,\gamma}_{\beta,\theta}$ *does not contain a positive vertex, then* Λ *does not contain an oriented* (α, γ)*-cycle.*

Proof. Assume that we have an oriented (α, γ)-cycle. Let τ be an innermost one which bounds a disk D_τ in D_Λ.

If there are vertices in $\mathrm{int}D_\tau$, one can find an oriented sequence σ of (α, γ)-edges in $\overline{D_\tau}$, which joins two vertices of τ (otherwise σ is an oriented (α, γ)-cycle). This sequence divides D_τ into two subdisks; the boundary of one of them is an oriented (α, γ)-cycle, contradicting the minimality of τ. Thus there is no vertex in $\mathrm{int}D_\tau$.

We call a *diagonal edge* in D_τ an edge of G_T in $\overline{D_\tau}$ which is not in τ. If there is a diagonal (α,γ)-edge e, then e divides D_τ into two subdisks; the boundary of one of them is an oriented (α,γ)-cycle, contradicting the minimality of τ. Hence there is no diagonal (α,γ)-edge in $\mathrm{int}D_\tau$. If there is no diagonal edge then the vertex v_τ of Γ corresponding to D_τ satisfies $I(v_\tau)=1$, i.e. v_τ is a positive vertex of Γ.

Note that each vertex in τ is incident to no diagonal edges or exactly two diagonal edges, because the cycle is oriented, see Figure 34.

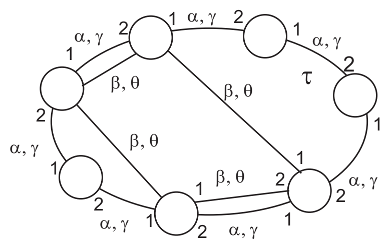

Figure 34

Therefore, if there is a diagonal edge then G_T contains a cycle in D_τ consisting of diagonal edges, each of which is a (β,θ)-edge. This then implies that the disk face bounded by this cycle corresponds to a dual vertex v with $I(v)=1$, i.e., v is a positive vertex of $\Gamma^{\alpha,\gamma}_{\beta,\theta}$. □

In particular, τ is not an oriented (α,γ)-cycle. We assume that τ is an innermost (α,γ)-cycle as above, which bounds a disk D_τ. Since τ is innermost, there are no vertices in $\mathrm{int}D_\tau$, for otherwise, we can find a smaller (α,γ)-cycle in D_τ. An edge of G_T in $\overline{D_\tau}$ which is not in τ is called a *diagonal edge* in D_τ. Since τ is innermost, every diagonal edge is a (β,θ)-edge. If $n\neq 0$, we denote by Y_1 (resp. Y_2) the vertices in τ incident to e_1 and ε_1 (resp. e_m and ε_n). If $n=0$ (i.e., $\tau=\partial_\Lambda f_0$), then we put $Y_i=X_i$ $(i=1,2)$.

Since $\partial_\Lambda f_0$ is a (α,γ)-cycle, a β-edge and a θ-edge appear only as an interior edge. Furthermore, since the θ-family is assumed to be non-empty, each black disk face contains a β-edge and a θ-edge on its boundary (because the black disk faces all are isomorphic).

Claim 7.8. *Λ has neither a white $<\gamma,\theta>$-corner nor a white $<\theta,\gamma>$-corner. In particular, Λ does not contain a disk face bounded by a (γ,θ)-cycle.*

Proof. Suppose first that the α-family is successive to the θ-family. Recall that ∂f contains $<\alpha,\beta>$-corner and a $<\beta,\alpha>$-corner. Then as in Figure 35, there is neither a white $<\theta,\gamma>$-corner nor a white $<\gamma,\theta>$-corner.

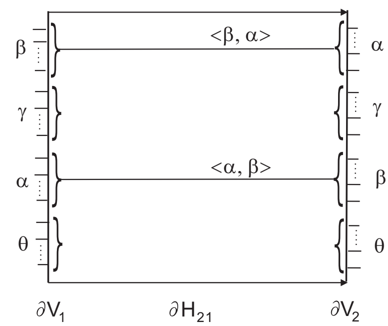

Figure 35

So we assume that the α-family is successive to the β-family.

Let p_i $(i = 1,2)$ be the endpoint of the ghost edge incident to X_i. Exchanging X_1 by X_2, if necessary, we may assume that p_i lies in ∂V_i.

Following [12], we say that an edge of Λ is *extremal* if the corresponding edge of G_T does not lie strictly between parallel edges of G_T (edges are parallel if they lie in the same isotopy class relative to ∂T). By Theorem [12, Theorem 2.1], G_D contains a great web Λ such that all ghost edges are extremal. The fact that Λ is innermost is self-contained in the proof of [12, Theorem 2.1]. In all the following, we assume that we choose such an innermost and extremal great web.

Recall that $\partial_\Lambda f_0$ is a (α,γ)-cycle, and the interior edges incident to X_1 and X_2 are (β,θ)-edges (Figure 36 (i)). On the other hand the boundary edges incident to X_1 (resp. X_2) are (α,γ)-edges both labeled by 2 (resp. 1). Therefore all the labels appear on ∂V_2 (resp. ∂V_1) among the successive (α,γ)-edges; in particular the label x_2 corresponding to X_2 (resp. the label x_1 corresponding to X_1) which is precisely p_2 (resp. p_1). Furthermore Λ

is extremal, thus the endpoints p_i lie between the α-family and the γ-family around ∂V_i, possibly in their boundary : see (Figure 36 (ii)). To be more precise, consider the corner around ∂V_i between the α-family and the γ-family ; then p_i lies in the closure of this family.

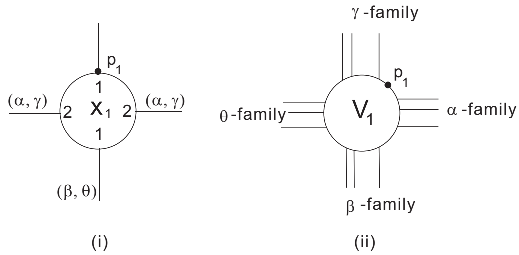

Figure 36

There is an alternating sequence of corners and edges in $\partial_\Lambda f_0$ joining p_1 to p_2 which is a part of the boundary of the white face in G_D just outside of Λ. Thus we have a white corner connecting p_1 and an endpoint of (α,γ)-edge ($< p_1, \alpha$ or $\gamma >$-corner) and a white corner connecting an endpoint of (α,γ)-edge and p_2 ($< \alpha$ or $\gamma, p_2 >$-corner). An existence of white $< p_1, \alpha$ or $\gamma >$-corner is an obstruction to an existence of white $< \gamma, \theta >$-corner, and similarly an existence of white $< \alpha$ or $\gamma, p_2 >$-corner is an obstruction to an existence of white $< \theta, \gamma >$-corner, see Figure 37.

Assume that Λ contains a disk face h bounded by a (γ,θ)-cycle. Since each black disk face should have a β-edge, h is a white disk face. Then ∂h contains white ($< \gamma, \theta >$ and $< \theta, \gamma >$)-corners, a contradiction. □

From Claim 7.8, we see that there is no θ-edge parallel to a boundary edge. If we have such a θ-edge, then we have a bigon bounded by an (α,θ)-cycle or a (γ,θ)-cycle. In either case the bigon would be white (because it has no β-edge). However the former possibility contradicts Claim 7.1 and the latter possibility contradicts Claim 7.8.

A vertex of τ incident to an ϵ_i edge is called *interior vertex of* τ. Since the sequence of interior edges of τ is oriented we have the following property:

The interior vertices of τ are incident to no diagonal edges or exactly two diagonal edges, and the boundary vertices other than $\{Y_1, Y_2, X_1, X_2\}$ are incident to exactly two diagonal edges. If X_i lies between Y_1 and Y_2,

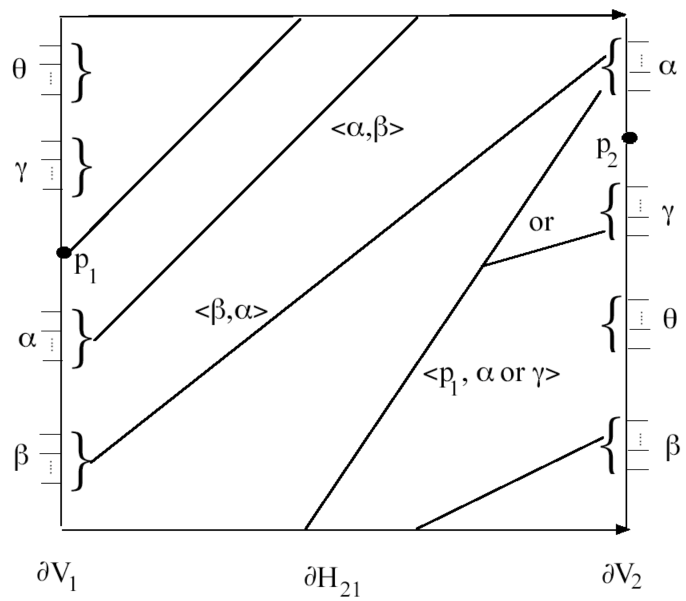

Figure 37

then exactly one interior edge is incident to X_i ($i = 1$ or 2). For simplicity, we call this *Property* (τ).

We may assume that there is no (β, θ)-cycle in D_τ, because it represents a positive vertex of $\Gamma^{\alpha,\gamma}_{\beta,\theta}$, contradicting the initial assumption of Lemma 7.5.

Since τ is not an oriented (α, γ)-cycle (Claim 7.7), τ contains at least two boundary vertices, and hence a boundary edge.

Claim 7.9. *There is a θ-edge in D_τ.*

Proof. Since τ is not an oriented cycle, there is a diagonal edge in D_τ. Thus D_τ contains a black disk face, which has a β-edge and θ-edge in its boundary. □

Let e_0 be a θ-edge in D_τ joining two vertices. Then e_0 divides D_τ into two subdisks D^1_τ and D^2_τ. At least one of them, say D_1, contains a boundary edge. If D_1 contains an interior θ-edge e_1, then e_1 divides D^1_τ into two subdisks D^1_1 and D^1_2; one of them (say D^1_1) contains a boundary edge. We repeat the process until we get an outermost θ-edge e. Then e divides D_τ into two subdisks; say D_1 and D_2 for convenience. First, we want to show that both contain a boundary edge. Assume that D_1 does not contain a boundary edge. By Property (τ) if one interior vertex in D_1 is incident to a diagonal edge (distinct to e) then D_1 contains a (β, θ)-cycle; a contradiction. Then D_1 is a disk face. Since all black disk faces are isomorphic and contain a β-edge, D_1 is white. By Claim 7.8, the edges adjacent to e around D_1 are α-edges. By Proposition 3.10 (i) $\rho(D_1) \neq \alpha^p\theta$ (where p is an integer); thus ∂D_1 contains a γ-edge. Since all black disk faces are isomorphic, all black disk faces contain an α-edge and a γ-edge on their boundaries. Consider now the black disk face incident to e. By Property (τ), its boundary contains at most one edge which is not a diagonal edge; this is a contradiction because diagonal edges are (β, θ)-edges and there is no (β, θ)-cycle.

Then, by an outermost argument, we may assume that an outermost θ-edge e divides D_τ into two subdisks D_1 and D_2, such that D_1 contains a boundary edge, but does not contain another θ-edge. By the isomorphism of black disk faces, either D_1 is a white disk face, or D_1 contains a single black disk face (which contains the θ-edge e on its boundary) and possible white disk faces.

Claim 7.10. *If h is a disk face of τ, then ∂h contains at most one boundary edge.*

Proof. Let h be a disk face of τ. Assume for a contradiction that ∂h contains two distinct boundary edges e_1 and e_2. By the Property (τ) they are not successive around ∂h. Therefore h does not satisfy Lemma 7.2 (3); which is a contradiction. □

Claim 7.11. *The disk D_1 is not a white disk face.*

Proof. Let e' be a boundary edge on ∂D_1. Assume for a contradiction that D_1 is a white disk face. By Claim 7.10 D_1 contains a single boundary edge e'. Since the θ-edge e is not parallel to the boundary edge e', ∂D_1 has length at least three. If neither endpoint of e is incident to a boundary vertex, then it turns out that τ is oriented, a contradiction. Thus exactly one endpoint of e is incident to a boundary vertex U; U is incident to both e and e'. Hence ∂D_1 consists of successive family of edges e, e' and interior edges $\varepsilon_1, \dots, \varepsilon_k$ (or $\varepsilon_k, \dots, \varepsilon_m$). By Claim 7.8 both edges successive to e are α-edges. Thus ∂D_1 contains an interior α-edge. Since black disk faces of Λ are isomorphic, this then implies that each black disk face has an α-edge on its boundary.

Let h be the black disk face having e on its boundary. Let $\eta_1, \ldots, \eta_k$ be the sequence of the successive edges around ∂h such that both η_1 and η_k are successive to e and that η_1 is incident to the boundary vertex U and η_k is incident to the interior vertex V (where V is the vertex incident to e and distinct to U, see Figure 38).

If $\eta_1, \ldots, \eta_k$ are diagonal edges, then ∂h is a (β, θ)-cycle, a contradiction. Hence η_i is not a diagonal edge for some i (so lies in τ). Note also that since V is an interior vertex, η_k is an interior edge, and hence η_1 joins U to a boundary vertex, otherwise ∂h consists of only diagonal edges (by Property (τ)) a contradiction; see Figure 38.

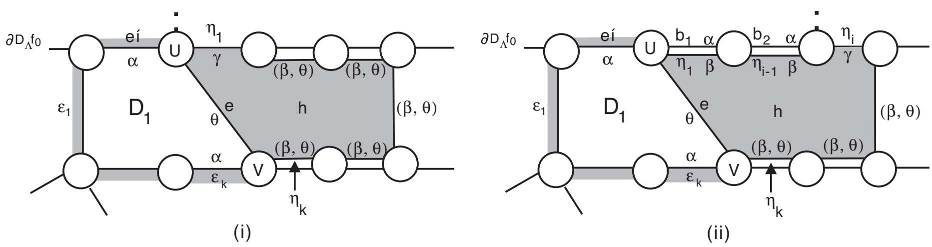

Figure 38

Suppose first that η_1 is a boundary edge (Figure 38 (i)). Then by Claim 6.2 η_1 is a γ-edge and U is X_1 or X_2.

Note that η_2 cannot be a boundary edge (Claim 7.10). Since (β, θ)-edges are successive on ∂h (Lemma 7.2 (3)), $\eta_2, \ldots, \eta_k$ are diagonal (β, θ)-edges. Hence ∂h has no α-edge, a contradiction.

Next suppose that $\eta_1, \ldots, \eta_{i-1}$ are diagonal (β, θ)-edges and η_i is a boundary edge (Figure 38 (ii)). Let D_3 be a subdisk of D_2 cut off by η_1 which does not contain h. We want to show that D_3 is a bigon. Assume that the length of ∂D_3 is greater than two. Since n_i is a boundary edge $(i > 1)$ then η_j joins boundary vertices, for $1 \leq j \leq i$; by Property (τ) and the fact that V is an interior vertex. Then the vertices on D_3 all are boundary vertices. Now we look at the Property (τ). According to whether some of these vertices lies in $\{X_1, X_2\}$ or not, either we can find a (β, θ)-cycle inside D_3, or, D_3 contains a black bigon adjacent to boundary edge (recall that a black bigon implies the required result, the existence of a black face with the support in an annulus). In both cases, we get a contradiction. Hence D_3 is a (white) bigon consisting of η_1 and a boundary edge b_1. Since a θ-edge is not parallel to a boundary edge, η_1 is a β-edge. If b_1 is a γ-edge, then D_3 is a primitive disk face with $\rho(D_3) = \beta\gamma$. Then Claim 7.1 shows that D_3 would be black, a contradiction. Thus b_1 is an α-edge, see Figure 38 (ii). Similarly η_j (for $1 \leq j < i$) cobounds a bigon with a boundary edge b_j; η_j is a β-edge and b_j is an α-edge. This then implies that η_i is a γ-edge (Claim 6.2). By Property (τ), V has two diagonal edges, then η_k is a diagonal edge which joins V to another vertex (because η_i is the single boundary edge of h). Repeating the same argument to this vertex, we conclude the same result for η_{k-1}, and so on until η_{i+1}. Hence, $\eta_{i+1}, \dots, \eta_k$ are (β, θ)-edges. Therefore ∂h does not have an α-edge, a contradiction. It follows that D_1 is not a white disk face. $\square$

Thus D_1 contains a single black disk face h and possible white disk faces.

Let us denote $\eta_1, \eta_2, \dots, \eta_k$ the successive edges on ∂h; η_1 is the outermost θ-edge e connecting two vertices U and V, η_2 is incident to U and η_k is incident to V.

Claim 7.12. *∂h has a boundary edge.*

Proof. Assume for a contradiction that ∂h does not have a boundary edge.

Recall that diagonal edges are (β, θ)-edges, and that there is no (β, θ)-cycle in D_τ.

Assume first that both U and V are interior vertices. Then D_τ contains a cycle σ consisting of e and additional interior edges. This cycle bounds a disk D_σ inside D_τ. By Property (τ) if one interior vertex in D_σ is incident to a diagonal edge then D_σ contains a (β, θ)-cycle; a contradiction. Then D_σ is a disk face. Since all black disk faces are isomorphic and contain a β-edge, D_σ is white. Therefore (Property (τ)) U is incident to another diagonal edge e_1 (distinct to e) in ∂h; similarly for V. Now, we apply successively the Property (τ) to the vertices incident to the edges around ∂h from $e, e_1, \dots$ to get that ∂h contains only diagonal edges (because we assume that ∂h does not contain a boundary edge).

Similarly, if both U and V are boundary vertices, then from Property (τ), we see that ∂h is a (β, θ)-cycle or we have another black disk face in D_1.

So we assume U is a boundary vertex and V is an interior vertex. Then there are two possibilities: η_k (incident to V) is a diagonal edge, or η_k is lying on ∂D_τ.

Now we show that the latter case cannot happen. For otherwise, V is incident to another diagonal edge e' in $D_\tau - D_1$ by Property (τ). Let $g(\subset D_\tau - D_1)$ be the white disk face containing e and e' on its boundary. By Claim 7.10 g has a single boundary edge e'' incident to U. Again by Property (τ), ∂g is the union of e'' and diagonal edges (because e, e' are diagonal edges, we repeat the same argument as above). If ∂g does not have a β-edge, then by Claim 7.8 $\rho(g) = \alpha\theta^x$ for some positive integer x. Then Claim 7.1 shows that g would be black, a contradiction. Thus ∂g has a β-edge, and hence, ∂g contains an $< \alpha, \theta >$-corner and a $< \theta, \beta >$-corner (or a $< \beta, \theta >$-corner and a $< \theta, \alpha >$-corner). However Figures 35 and 37 show that it is impossible.

Thus η_k is a diagonal edge. Then since ∂h has no boundary edge, we see (Property (τ)) that ∂h is a (β, θ)-cycle; a contradiction. $\square$

Claim 7.13. *$\rho(h) = \theta\beta^a\gamma\beta^b$, up to orientation and cyclic permutation, for some integers $a > 0$ and $b \geq 0$.*

Proof. By the previous claim, ∂h has a boundary edge. Then by Claim 7.10 it has exactly one boundary edge; in particular, it has at least two boundary vertices.

Let W_i be the vertex incident to η_i and η_{i+1} so that $W_1 = U$ and $W_k = V$.

Recall that diagonal edges in D_1 other than e are β-edges and ∂h is the union of a sequence of successive (β, θ)-edges and a sequence of successive (α, γ)-edges (Lemma 7.2 (3)). Since ∂h has a β-edge and the boundary edge is an (α, γ)-edge, η_2 or η_k is a β-edge. We may assume (if necessary by taking the opposite order of $\eta_2, \ldots, \eta_k$ so that the roles of η_2 and η_k is exchanged) η_2 is a diagonal β-edge. Let us assume that $\eta_2, \eta_3, \ldots, \eta_i$ be successive diagonal β-edges (possibly $i = 2$). Since ∂h is not a (β, θ)-cycle, there exists i such that η_{i+1} is not a diagonal edge. If W_i is an interior vertex, then by Property (τ) D_1 contains another black disk face. So W_i is a boundary vertex and η_{i+1} is a boundary edge. Then W_{i+1} is also a boundary vertex and η_{i+2} is not a boundary edge (there is a single boundary edge on ∂h). Suppose that η_{i+2} is not a diagonal edge, then it lies on ∂D_τ. The absence of black disk faces other than h and Property (τ) imply that $\eta_{i+2}, \eta_{i+3}, \ldots, \eta_k$ are lying on ∂D_τ, see Figure 39.

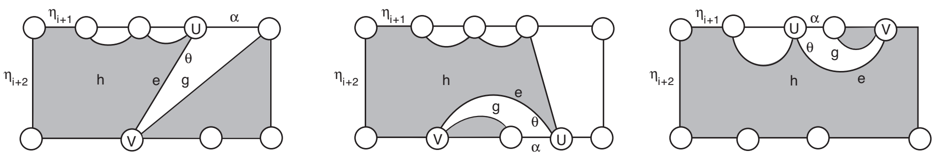

Figure 39

Then since $\eta_k \subset \partial D_\tau$, V is incident to another diagonal edge $e' \neq e$ and a white disk face $g(\subset D_\tau - D_1)$ as above. Applying the same argument in the proof of Claim 7.12, we have a contradiction. Therefore η_{i+2} is a diagonal edge; thus this is a β-edge.

Hence by Lemma 7.2 (3), $\eta_{i+3}, \dots, \eta_k$ are β-edges. Note that η_{i+2} is possibly $\eta_1 = e$.

If η_{i+1} is shown to be a γ-edge, then $\rho(h) = \theta\beta^a\gamma\beta^b$ for some positive $a > 0$ and $b \geq 0$.

Now let us show that η_{i+1} is a γ-edge.

All the vertices on ∂h are boundary vertices. Indeed, assume for a contradiction that ∂h contains a vertex Y which is not a boundary vertex, then $Y \notin \{W_i, W_{i+1}\}$. Hence the edges on ∂h incident to Y are (β, θ)-edges. Since all the vertices but X_1, X_2 are incident to (α, γ)-edges with both labels 1 and 2 (by Claim 7.6), Y is incident to a black face g such that ∂g contains at least two (α, γ)-edges; thus $\rho(h) \neq \rho(g)$ a contradiction.

Therefore, all the η_i's except $e = \eta_1$ bound a white face of length two on D_1 (because D_1 does not contain another black face).

Let $h'(\subset D_1)$ be the white disk face whose boundary contains η_i. Let e' be the edge around $\partial h'$, incident to W_i, and distinct from η_i. By Claim 7.1 e' is a α-edge. Thus η_{i+1} is a γ-edge by Claim 6.2, as desired. □

Claim 7.14. *The α-family is adjacent to the β-family.*

Proof. Assume for a contradiction that the α-family is adjacent to the θ-family. As in the proof of Claim 7.8, we take a sequence of alternating sequence of corners and edges of $\partial_\Lambda f_0$ joining p_1 to p_2 which is a part of the boundary of the disk face in G_D just outside of Λ. (This black face is the opposite side of the white face used in the the proof of Claim 7.8.) Thus we have a black corner connecting p_1 and an endpoint of (α, γ)-edge ($< p_1, \alpha$ or $\gamma >$-corner) and a black corner connecting an endpoint of (α, γ)-edge and p_2 ($< \alpha$ or $\gamma, p_2 >$-corner). Hence Λ cannot contain the black corners given by the black disk face h (Claim 7.13), see Figure 40 (i) if $\rho(h) = \theta\beta^a\gamma$ (i.e., $b = 0$) and Figure 40 (ii) if $\rho(h) = \theta\beta^a\gamma\beta^b$ (i.e., $b > 0$). $\square$

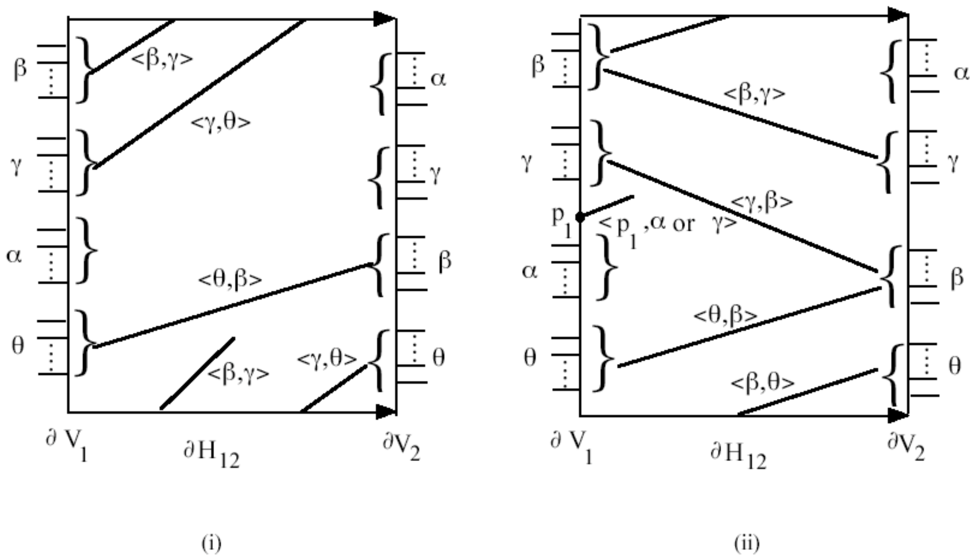

Figure 40

Claim 7.15. *There exists a white corner which is either a $< \theta, \beta >$-corner, a $< \beta, \theta >$-corner or a $< \theta >$-corner.*

Proof. Let g be the white face having e on its boundary; g is the opposite side of h along e. Let e_U, e_V be the edges adjacent to e on ∂g, and incident to U and V respectively. If one of them is a diagonal edge, then we obtain the required result. So we may assume that they are both α-edges by Claim 7.8. Since black disk faces are isomorphic (Proposition 3.9 (i)), Claim 7.13 implies that the α-edges are boundary edges. By Claim 7.10 $e_U = e_V$, and hence g is a white primitive disk face with $\rho(g) = \alpha\theta$. Then by Claim 7.1 g would be black; a contradiction. $\square$

By Claim 7.14 the α-family is adjacent to the β-family. Then from Figure 37, we see that Λ cannot contain a white corner which is a $< \theta, \beta >$-corner, a $< \beta, \theta >$-corner or a $< \theta >$-corner. However this contradicts Claim 7.15. This completes the proof of Lemma 7.5. $\square$

If the family of θ-edges is adjacent to the family of the α-edges, then we have the following result; the proof is identical by replacing notations.

Addendum 7.16. *Assume that the family of θ-edges is adjacent to the family of the α-edges. If there is no black disk face whose the support lies in an annulus in $\widehat{T}$, then there exists a positive vertex in $\Gamma^{\alpha,\theta}_{\beta,\gamma}$ (for which (α, θ)-edges are BW and (γ, β)-edges are WB).*

Suppose for a contradiction that Λ does not have a black disk face whose support is contained in an annulus in $\hat{T}$. Then by Lemma 7.5, we have a positive vertex in $\Gamma^{\alpha,\gamma}_{\beta,\theta}$. Let g be the corresponding disk face of Λ, which would be white. Then ∂g is either an (α, γ)-cycle or a (β, θ)-cycle. We assume, if necessary changing α (resp. γ) with β (resp. θ), that ∂g is an (α, γ)-cycle.

Claim 7.17. *There exists a positive vertex in $\Gamma^{\alpha}_{\beta,\gamma,\theta}$ (in which an α-edge is BW and a (β, γ, θ)-edge is WB).*

Proof. Assume for a contradiction that $\Gamma^{\alpha}_{\beta,\gamma,\theta}$ does not contain a positive vertex. Notice that the BW-edges are successive around ∂V_i (for $i = 1$ or 2) since they are α-edges, and similarly for the WB-edges (since they are the edges which are not the α-edges); so we can apply Lemma 7.2. By Lemma 7.2 (3) the α-edges (resp. γ-edges) are successive around ∂g. Thus $\partial g = \alpha^m \gamma^n$ for some positive integers m, n. We may assume $m, n \geq 2$, for otherwise, g is primitive and Claim 7.1 shows that g would be black, a contradiction. Thus we have an $< \alpha >$-corner and a $< \gamma >$-corner in ∂g. Hence the white corners are given as in Figure 41 (i) (ii) depending on whether the β-family is adjacent to the α-family or not.

Then, for any edge class label δ, each white $< \delta, \theta >$-corner (resp. $< \theta, \delta >$-corner) is an $< \alpha, \theta >$-corner (resp. $< \theta, \alpha >$-corner). Since there is a θ-edge, we have a white face h so that ∂h contains a θ-edge e. Now assume for a contradiction that h is not a disk face (i.e., h is the annulus face f_0); h is divided into a black disk and a white disk by two ghost edges. Since $\partial_\Lambda f_0$ is a (β, γ, θ)-cycle (Lemma 7.2(2) and (4)), e joins X_1 and X_2, for otherwise, we would have a white corner in $h = f_0$ which

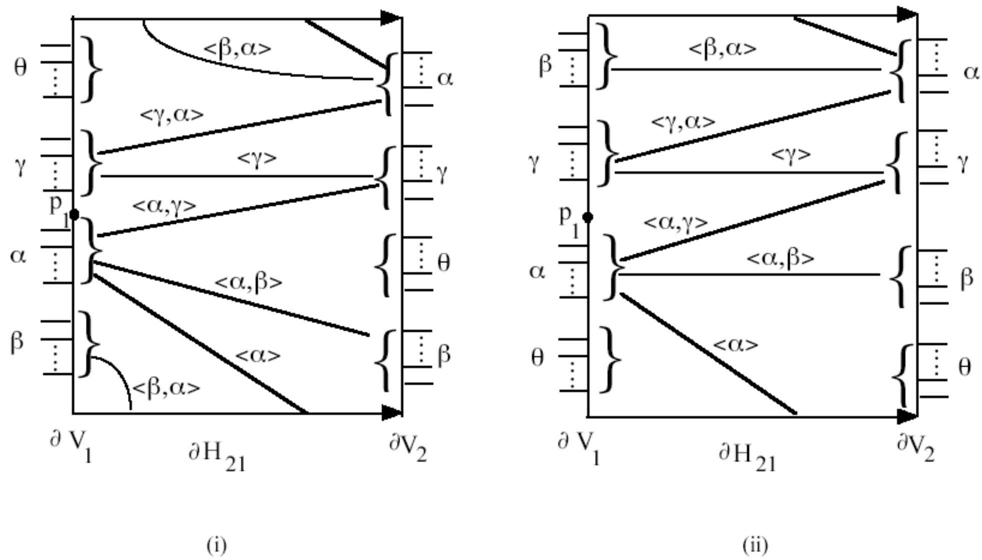

FIGURE 41

is neither an $< \alpha, \theta >$-corner nor a $< \theta, \alpha >$-corner. This means that there is a $< p_1, \theta >$-corner, where p_1 is the endpoint of the ghost edge incident to X_1. However this is impossible; see Figure 41. It follows that h is a white disk face with $\rho(h) = \cdots \alpha\theta\alpha \cdots$. Then by Lemma 7.2 (3), $\rho(h) = \alpha^2\theta$, hence h is primitive. Thus Claim 7.1 shows that h would be black, a contradiction. $\square$

'Let h be the disk face of Λ corresponding to the positive vertex in $\Gamma^{\alpha}_{\beta,\gamma,\theta}$. Note that ∂h is a (β, γ, θ)-cycle by Lemma 3.4.

Claim 7.18. *The disk face h is black.*

Proof. Assume that h is white. Since the white disk face g gives white $< \alpha, \gamma >$-corners and white $< \gamma, \alpha >$-corners in ∂g, we have white corners as in Figure 41 with the $< \alpha >$-corners and the $< \gamma >$-corners removed. This then implies that if ∂h contains a γ-edge, then since ∂h is a (β, γ, θ)-cycle and it does not have an α-edge, ∂h is a γ-cycle (i.e., there are only

$<\gamma>$-corners in ∂h). This contradicts Lemma 3.4. Thus ∂h is a (β, θ)-cycle, and hence there are white $<\beta, \theta>$-corners and white $<\theta, \beta>$-corners. However it is impossible if the β-family is adjacent to the α-family, see Figure 41 (i) with the $<\alpha>$-corners and the $<\gamma>$-corners removed. So we may assume that the θ-family is adjacent to the α-family, see Figure 42 below.

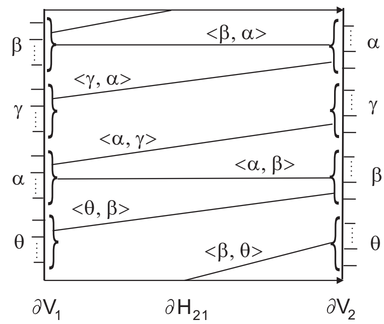

Figure 42

Let us recall from Addendum 7.16 that $\Gamma^{\alpha,\theta}_{\beta,\gamma}$ has a positive vertex. We may assume that the corresponding disk face h' is white. Then $\partial h'$ contains either a white $<\alpha, \theta>$-corner or a white $<\beta, \gamma>$-corner, which is impossible, see Figure 42. $\square$

Since the black disk face h is bounded by a (β, γ, θ)-cycle and the black disk faces all are isomorphic (Proposition 3.9 (i)), the α-edges cannot be interior edges, i.e., they are boundary edges. By Claim 7.10, $\rho(g) = \alpha\gamma^n$ for some positive integer n, i.e., g is primitive. Then Claim 7.1 shows that g would be black, a contradiction. This completes the proof of Proposition 3.10 (ii) in Case 1.

7.3. **Proof of Proposition 3.10–Case 2**

In this subsection, we prove Proposition 3.10 (ii) under the assumption: *The γ-family or the θ-family is empty.*

If the γ-family and the θ-family are both empty, then the support of a black disk face is in an annulus in $\hat{T}$. So we may assume that Λ contains a γ-edge or a θ-edge. In the following, if necessarily changing θ with γ, we assume that there is no θ-edge in Λ. Note that in the present situation, any two distinct families are adjacent around ∂V_1. Now let us choose oriented dual graphs $\Gamma^{\alpha}_{\beta,\gamma}$ (in which α-edge is BW, β,γ-edge is WB) and $\Gamma^{\beta}_{\alpha,\gamma}$ (for which a β-edge is BW and an (α,γ)-edge is WB).

Claim 7.19. *Either $\Gamma^{\alpha}_{\beta,\gamma}$ or $\Gamma^{\beta}_{\alpha,\gamma}$ contains a positive vertex. Moreover if both $\Gamma^{\alpha}_{\beta,\gamma}$ and $\Gamma^{\beta}_{\alpha,\gamma}$ have positive vertices, then Λ contains a required black disk face whose support lies in an annulus in $\hat{T}$.*

Proof. First assume for a contradiction that neither $\Gamma^{\alpha}_{\beta,\gamma}$ nor $\Gamma^{\beta}_{\alpha,\gamma}$ contains a positive vertex. By Lemma 7.2 (4), $\partial_\Lambda f_0$ is not a δ-cycle for $\delta \in \{\alpha,\beta,\gamma\}$. Furthermore (Lemma 7.2 (2)) $\partial_\Lambda f_0$ is a (β,γ)-cycle and simultaneously a (α,γ)-cycle, so it is a γ-cycle, a contradiction.

Next suppose that both $\Gamma^{\alpha}_{\beta,\gamma}$ and $\Gamma^{\beta}_{\alpha,\gamma}$ contain positive vertices. Let g, h be the corresponding disk faces in Λ respectively. Then we may assume that g, h are not black, because their support are in an annulus in $\hat{T}$. Thus the family of white corners contains:
an $<\alpha,\beta>$-corner and a $<\beta,\alpha>$-corner on ∂f; and
a $<\beta,\gamma>$-corner and a $<\gamma,\beta>$-corner on ∂g; and
an $<\alpha,\gamma>$-corner and a $<\gamma,\alpha>$-corner on ∂h.

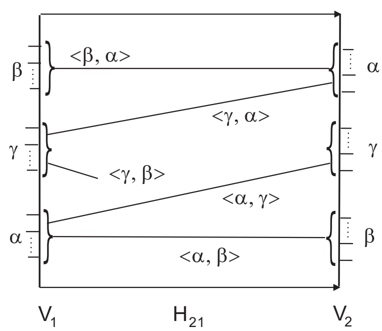

Figure 43

This is impossible, see Figure 43. □

To prove Proposition 3.10 (ii) (in Case 2), we assume, without loss of generality, that $\Gamma^{\beta}_{\alpha,\gamma}$ has a positive vertex, but $\Gamma^{\alpha}_{\beta,\gamma}$ does not have a positive vertex. Let h be the disk face of Λ corresponding to a positive vertex of

$\Gamma^{\beta}_{\alpha,\gamma}$. Then ∂h is an (α,γ)-cycle (Lemma 3.4). Lemma 7.2 shows that $\partial_\Lambda f_0$ is a (β,γ)-cycle and $\rho(h) = \alpha^m\gamma^n$ for some positive integers m, n. We may assume that $m, n \geq 2$, for otherwise g is primitive and Claim 7.1 shows that g would be black, a contradiction. Therefore we have a white $<\alpha>$-corner, a white $<\alpha,\gamma>$-corner, a white $<\gamma>$-corner and a white $<\gamma,\alpha>$-corner.

Recall that the edges of G_D incident to the ghost labels at X_1 and X_2 divide f_0 into a black disk D_B and a white disk D_W. The edges of $\partial_\Lambda f_0$ in D_B (resp. D_W) is said to be *black* (resp. *white*).

Claim 7.20. *All the white edges in $\partial_\Lambda f_0$ are γ-edges, or there exists a black disk face whose support lies in an annulus in $\hat{T}$.*

Proof. Recall that $\partial_\Lambda f_0$ is a (β,γ)-cycle. Assume that $\partial_\Lambda f_0$ contains a white β-edge e. Then e joins X_1 to X_2, for otherwise we have a white $<\beta,\delta>$-corner or a white $<\delta,\beta>$-corner in $D_W \subset f_0$ with $\delta = \beta$ or γ, which is impossible, see Figure 44.

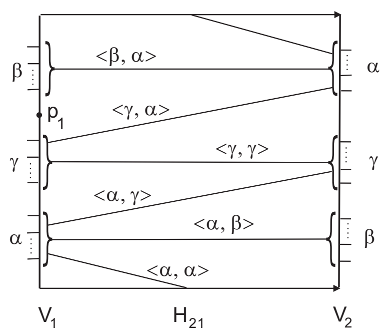

Figure 44

Let h be the black disk face adjacent to e. Since the interior edges incident to X_1 and X_2 are α-edges (Lemma 7.2 (2)) and β-edges and γ-edges (WB-edges) are successive (Lemma 7.2 (3)), $\rho(h) = \beta\alpha^n$ for some integer n. Hence h is a black disk face whose support lies in an annulus in $\hat{T}$. $\square$

It follows that we may assume that all the white edges in $\partial_\Lambda f_0$ are γ-edges. Then there exists a white $<p_1,\gamma>$-corner, where p_1 is the endpoint of the ghost edge labeled by 1 on ∂X_1 or ∂X_2. Moreover by Claim 6.2, p_1 is lying between the γ-family and the β-family (cf. Figure 36 with α and β changed). However this is impossible, see Figure 44.

This completes the proof of Propositon 3.10 (ii) in Case 2.

References

[1] M. Aït Nouh, D. Matignon et K. Motegi – Obtaining graph knots by twisting unknots, *C. R. Acad. Sci. Paris, Ser. I* **337** (2003), p. 321–326.

[2] ———, Obtaining graph knots by twisting unknots, *Topology Appl.* **146-147** (2005), p. 105–121.

[3] M. Culler, J. L. C. McA. Gordon et P. B. Shalen – Dehn surgery on knots, *Ann. Math* **125** (1987), p. 237–300.

[4] L. Glass – A combinatorial analog of the Poincaré index theorem, *J. Comb. Theory Ser.* **B15** (1973), p. 264–268.

[5] H. Goda, C. Hayashi et H.-J. Song – Dehn surgeries on 2-bridge links which yield reducible 3-manifolds, preprint.

[6] C. Goodman-Strauss – On composite twisted unknots, *Trans. Amer. Math. Soc.* **349** (1997), p. 4429–4463.

[7] C. Gordon – Combinatorial methods in Dehn surgery, Lectures at Knots 96, World Scientific Publishing Co, 1997, p. 263–290.

[8] C. Gordon et R. A. Litherland – Incompressible planar surfaces in 3-manifolds, *Topology Appl.* **18** (1984), p. 121–144.

[9] C. Gordon et J. Luecke – Knots are determined by their complements, *J. Amer. Math. Soc.* **2** (1989), p. 371–415.

[10] ———, Dehn surgeries on knots creating essential tori, I, *Comm. Anal. Geom.* **4** (1995), p. 597–644.

[11] ———, Toroidal and boundary-reducing Dehn fillings, *Topology Appl.* **93** (1999), p. 77–90.

[12] ———, Non-integral toroidal Dehn surgeries, *Comm. Anal. Geom.* **12** (2004), p. 417–485.

[13] C. Hayashi et K. Motegi – Only single twist on unknots can produce composite knots, *Trans. Amer. Math. Soc.* **349** (1997), p. 4465–4479.

[14] W. Jaco et P. B. Shalen – Seifert fibered spaces in 3-manifolds, *Mem. Amer. Math. Soc.* **220** (1979).

[15] K. Johannson – *Homotopy equivalences of* 3*-manifolds with boundaries*, Lect.Notes in Math, Springer-Verlag, 1979.

[16] M. Kouno, K. Motegi et T. Shibuya – Twisting and knot types, *J. Math. Soc. Japan* **44** (1992), p. 199–216.

[17] Y. Mathieu – Unknotting, knotting by twists on disks and property (P) for knots in s^3, *Knots 90 (ed. by Kawauchi), Proc. 1990 Osaka Conf. on Knot Theory and Related Topics, de Gruyter* (1992), p. 93–102.

[18] W. Menasco – Closed incompressible surfaces in alternating knot and link complements, *Topology* **23** (1984), p. 37–44.

[19] K. Miyazaki et K. Motegi – Seifert fibered manifolds and Dehn surgery III, *Comm. Anal. Geom.* **7** (1999), p. 551–582.

[20] J. Morgan et H. Bass – *The Smith conjecture*, Academic Press, 1984.

[21] K. Motegi – Knot types of satellite knots and twisted knots, Lectures at Knots 96, World Scientific Publishing Co, 1997, p. 579–603.

[22] K. Motegi et T. Shibuya – Are knots obtained from a plain pattern always prime ?, *Kobe J. Math.* **9** (1992), p. 39–42.

[23] Y. Ohyama – Twisting and unknotting operations, *Rev. Mat. Univ. Complut. Madrid* **7** (1994), p. 289–305.

[24] D. Rolfsen – *Knots and links*, Publish or Perish, Berkeley, Calif., 1976.

[25] M. Scharlemann – Unknotting-number-one knots are prime, *Invent. Math.* **82** (1985), p. 37–55.

[26] ———, Producing reducible 3-manifolds by surgery on a knot, *Topology* **29** (1990), p. 481–500.

[27] M. Teragaito – Composite knots trivialized by twisting, *J. Knot Theory Ramifications* **1** (1992), p. 1623–1629.

[28] W. P. Thurston – *The geometry and topology of* 3*-manifolds*, Lecture notes, Princeton University, 1979.

[29] Y.-Q. Wu – Dehn surgery on arborescent links, *Trans. Amer. Math. Soc.* **351** (1999), p. 2275–2294.

Mohamed Aït-Nouh
Department of Mathematics
University of California at Santa Barbara
Boston, MA 02215
USA
aitnouh@math.ucsb.edu

Daniel Matignon
CMI, UMR 6632 du CNRS
Université d'Aix-Marseille I
39, rue Joliot Curie
F-13453 Marseille Cedex 13
FRANCE
matignon@cmi.univ-mrs.fr

Kimihiko Motegi
Department of Mathematics
Nihon University
Tokyo 156-8550
JAPAN
motegi@math.chs.nihon-u.ac.jp